

COMPARISON OF AERMOD AND ISCST3 MODELS FOR PARTICULATE  
EMISSIONS FROM GROUND LEVEL SOURCES

A Thesis

by

VENKATA SAI VAMSI BOTLAGUDURU

Submitted to the Office of Graduate Studies of  
Texas A&M University  
in partial fulfillment of the requirements for the degree of  
MASTER OF SCIENCE

December 2009

Major Subject: Biological and Agricultural Engineering

COMPARISON OF AERMOD AND ISCST3 MODELS FOR PARTICULATE  
EMISSIONS FROM GROUND LEVEL SOURCES

A Thesis

by

VENKATA SAI VAMSI BOTLAGUDURU

Submitted to the Office of Graduate Studies of  
Texas A&M University  
in partial fulfillment of the requirements for the degree of

MASTER OF SCIENCE

Approved by:

Chair of Committee,	Calvin B. Parnell, Jr.
Committee Members,	Ronald E. Lacey
	Sergio Capareda
	Qi Ying
Head of Department,	Gerald L. Riskowski

December 2009

Major Subject: Biological and Agricultural Engineering

## ABSTRACT

Comparison of AERMOD and ISCST3 Models for Particulate Emissions from Ground Level Sources. (December 2009)

Venkata Sai Vamsi Botlaguduru, B.Tech, Acharya Nagarjuna University

Chair of Advisory Committee: Dr. Calvin B. Parnell, Jr.

Emission factors (EFs) and results from dispersion models are key components in the air pollution regulatory process. The EPA preferred regulatory model changed from ISCST3 to AERMOD in November, 2007. Emission factors are used in conjunction with dispersion models to predict 24-hour concentrations that are compared to National Ambient Air Quality Standards (NAAQS) for determining the required control systems in permitting sources. This change in regulatory models has had an impact on the regulatory process and the industries regulated.

In this study, EFs were developed for regulated particulate matter  $PM_{10}$  and  $PM_{2.5}$  from cotton harvesting. Measured concentrations of TSP and  $PM_{10}$  along with meteorological data were used in conjunction with the dispersion models ISCST3 and AERMOD, to determine the emission fluxes from cotton harvesting. The goal of this research was to document differences in emission factors as a consequence of the models used. The  $PM_{10}$  EFs developed for two-row and six-row pickers were  $154 \pm 43 \text{ kg/km}^2$  and  $425 \pm 178 \text{ kg/km}^2$ , respectively. From the comparison between AERMOD and ISCST3, it was observed that AERMOD EFs were 1.8 times higher than ISCST3 EFs for

a six-row harvester. This suggests that EFs for fugitive emissions developed using dispersion models are model specific.

In our research on EFs from cotton harvesting, we discovered that an alternative dispersion modeling protocol could be used to yield EFs. This new dispersion modeling approach was described and evaluated. The approach included modeling the harvesting operation as a series of line sources instead of a stationary area source.

A comparison of downwind concentrations predicted by AERMOD and ISCST3 from a hypothetical cattle feedlot with varying meteorological conditions and emission rates were evaluated. It was observed that pollutant concentration results for the two models were dependent upon solar radiation. The impacts of solar radiation on downwind concentrations using AERMOD were different than those obtained using ISCST3. Results using the two models were compared under different meteorological conditions and solar radiation ranges. The results indicate that there is a linear relation between the models for all conditions. These results demonstrate that AERMOD predicted concentrations 55% higher than ISCST3 in the absence of solar radiation. This study also included an evaluation of both models with actual downwind concentration measurements taken at a feedlot in the Texas panhandle. It was observed that both models over-predict concentrations in a rural flat terrain. AERMOD's performance was within acceptable limits for a convective and neutral atmosphere, but was not acceptable for a stable atmosphere. AERMOD predicted concentrations three times higher than the measured concentrations during night time conditions (zero solar radiation). The results indicate inconsistencies in the AERMOD model used to estimate concentrations in the

absence of solar radiation. Using AERMOD predictions of pollutant concentrations off property for regulatory purposes will likely affect a source's ability to comply with limits set forth by State Air Pollution Regulatory Agencies (SAPRAs) and could lead to inappropriate regulation of the source.

## DEDICATION

This thesis is dedicated to my parents and my brother, for the love and support they have shown.

## ACKNOWLEDGEMENTS

I would like to thank my committee chair, Dr. Calvin Parnell, Jr., for the guidance and support he gave to this research. Dr. Parnell, you have been a source of great inspiration. Your perspective of a professional engineer inspires students a lot. I will be forever in debt to you.

I would like to thank my committee members, Dr. Ron Lacey, Dr. Sergio Capareda and Dr. Qi Ying, for their support and advice throughout my graduate study.

Thanks to Dr. Brock Faulkner for his valuable suggestions, encouragement and guidance.

Thanks to Col. Russell McGee and to my colleagues in 324 Scoates Hall for their support and encouragement. I enjoyed working with you all. Thank you for making this time such a memorable experience.

Thanks to the Cotton Chair, Texas AgriLife Research for making this research possible.

Finally, but most importantly, I thank God for everything that he has made possible for me.

## TABLE OF CONTENTS

	Page
ABSTRACT .....	iii
DEDICATION .....	vi
ACKNOWLEDGEMENTS .....	vii
TABLE OF CONTENTS .....	viii
LIST OF FIGURES.....	x
LIST OF TABLES .....	xii
CHAPTER	
I INTRODUCTION.....	1
II EMISSION FACTORS FOR COTTON HARVESTING: A NEW APPROACH TO DISPERSION MODELING FOR HARVEST OPERATIONS.....	6
Introduction .....	6
Methodology .....	9
Results and Discussion.....	18
Conclusions .....	24
III COMPARISON OF AERMOD AND ISCST3 FOR EMISSIONS FROM A FEEDLOT .....	26
Introduction .....	26
Methodology .....	29
Hypothetical Source .....	29
Measured PM Concentrations at a Feedlot .....	33
Results and Discussion.....	38
Hypothetical Source .....	38
Measured PM Concentrations at a Feedlot .....	59
Conclusions .....	66



CHAPTER	Page
IV SUMMARY AND CONCLUSIONS.....	68
REFERENCES.....	71
APPENDIX A METEOROLOGICAL DATA FOR MODELING .....	74
APPENDIX B METEOROLOGICAL DATA PROCESSING FOR COTTON HARVESTING DATA .....	78
APPENDIX C METEOROLOGICAL DATA PROCESSING FOR FEEDLOT DATA .....	87
VITA .....	95

## LIST OF FIGURES

	Page
Figure 1. Schematic of the Flocchini box model.....	7
Figure 2. Layout of test plots .....	10
Figure 3. Method 1 setup in AERMOD .....	13
Figure 4. Method 2 setup in AERMOD .....	15
Figure 5. Model setup parameters .....	32
Figure 6. Cattle feedlot with a TEOM sampler .....	35
Figure 7. Wind rose for feedlot E.....	36
Figure 8. Regression plot for ISCST3 vs. AERMOD concentrations at the edge of the feedlot in a convective atmosphere.....	42
Figure 9. Regression plot for ISCST3 vs. AERMOD concentrations at the edge of the feedlot in a stable atmosphere.....	43
Figure 10. Regression plot for ISCST3 vs. AERMOD concentrations at the edge of the feedlot in a neutral atmosphere.....	44
Figure 11. Regression plot for ISCST3 vs. AERMOD concentrations at the edge of the feedlot when solar radiation is zero .....	45
Figure 12. Regression plot for ISCST3 vs. AERMOD concentrations at the edge of the feedlot when solar radiation $< 800 \text{ W/m}^2$ .....	46
Figure 13. Regression plot for ISCST3 vs. AERMOD concentrations at the edge of the feedlot when solar radiation $> 800 \text{ W/m}^2$ .....	47
Figure 14. Regression plot for ISCST3 vs. AERMOD concentrations at the edge of the feedlot in an urban convective atmosphere.....	49
Figure 15. Regression plot for ISCST3 vs. AERMOD concentrations at the edge of the feedlot in an urban stable atmosphere.....	50

Figure 16. Regression plot for ISCST3 vs. AERMOD concentrations at the edge of the feedlot in an urban neutral atmosphere.....	51
Figure 17. Regression plot for ISCST3 vs. AERMOD concentrations in an urban case at the edge of the feedlot when solar radiation is zero.....	52
Figure 18. Regression plot for ISCST3 vs. AERMOD concentrations in an urban case at the edge of the feedlot when solar radiation $< 800 \text{ W/m}^2$ .....	53
Figure 19. Regression plot for ISCST3 vs. AERMOD concentrations in an urban case at the edge of the feedlot when solar radiation $> 800 \text{ W/m}^2$ .....	54
Figure 20. Variance in AERMOD and ISCST3 concentrations as a function of wind speed.....	59
Figure 21. Scatter plot for measured vs. AERMOD concentrations when solar radiation $< 800 \text{ W/m}^2$ .....	63
Figure 22. Regression plot for measured vs. AERMOD concentrations during the night time .....	64

## LIST OF TABLES

	Page
Table 1. EFs in $\text{kg}/\text{km}^2$ for six-row harvester using Method 1 and 2.....	19
Table 2. EFs in $\text{kg}/\text{km}^2$ for two-row harvester using Method 1 and 2.....	19
Table 3. Correlation analysis of TSP EFs with process variables.....	20
Table 4. Correlation analysis of FRM $\text{PM}_{10}$ EFs with process variables.....	22
Table 5. Comparison of $\text{PM}_{10}$ EFs in $\text{kg}/\text{km}^2$ from AERMOD and ISCST3.....	23
Table 6. Comparison of source-sampling EFs and the EFs developed by dispersion models in $\text{kg}/\text{km}^2$ .....	24
Table 7. Correlation analysis.....	38
Table 8. Percent differences in AERMOD and ISCST3 concentrations at the edge of the feedlot under different atmospheric criteria.....	39
Table 9. Regression parameters for AERMOD vs. ISCST3 concentrations at the edge of the feedlot for rural surface roughness .....	41
Table 10. Regression parameters for AERMOD vs. ISCST3 concentrations at the edge of the feedlot for urban surface roughness.....	48
Table 11. Regression parameters for AERMOD vs. ISCST3 and rural surface roughness @ 500 m.....	55
Table 12. Regression parameters for AERMOD vs. ISCST3 and urban surface roughness @ 500 m .....	56
Table 13. Regression parameters for AERMOD vs. ISCST3 and rural surface roughness @ 1000 m.....	57
Table 14. Regression parameters for AERMOD vs. ISCST3 and urban surface roughness @ 1000 m .....	57
Table 15. NMSE and FB values for AERMOD under different atmospheric criteria .....	60

Page

Table 16. NMSE and FB values for ISCST3 under  
different atmospheric criteria .....60

## CHAPTER I

### INTRODUCTION

The Clean Air Act of 1970 formed the Environmental Protection Agency (EPA) (CFR, 1999). The act also required the EPA to establish National Ambient Air Quality Standards (NAAQS) for six criteria pollutants, sulfur dioxide (SO<sub>2</sub>), nitrogen dioxide (NO<sub>2</sub>), particulate matter (PM), carbon monoxide (CO), ozone (O<sub>3</sub>), and lead (Pb) (Cooper and Alley, 2002). Particulate matter is the primary pollutant of concern to the agricultural industry. Specifically, particulate matter with aerodynamic equivalent diameter (AED) less than 10 μm (PM<sub>10</sub>) and particulate matter with AED less than 2.5 μm (PM<sub>2.5</sub>) are the regulated pollutants. Areas with sufficient number of exceedances of the NAAQS for any pollutant are classified as non-attainment and state air pollution regulatory agencies (SAPRAs) must develop state implementation plans (SIP) to bring them into attainment. Some SAPRAs use NAAQS to limit the concentrations at the property line and beyond. Dispersion models are the tools used by SAPRAs to estimate off-property concentrations of pollutants from air pollution sources. The primary inputs to these models are emission rates and meteorological data. Concentrations predicted by dispersion models enable SAPRAs to impose further restrictions on the release of pollutants if required, and have a major effect on the operational permits of an industry.

---

This thesis follows the style of *Transactions of the ASABE*.

The EPA designated Industrial Source Complex: Short Term version 3 (ISCST3) as the preferred dispersion model for states to use in the regulation of air pollution sources prior to Dec, 2006. Subsequent to this date EPA designated the American Meteorological Society/Environmental Protection Agency Regulatory Model (AERMOD) as the preferred model. This change in preferred regulatory dispersion models could potentially impact the air pollution regulatory process and the industries regulated. Both models apply the same Gaussian equation to model the dispersion of pollutants, but they differ in the treatment of meteorological and land use data. These different treatments of input data result in significant differences in concentrations predicted by the models. Several studies have been conducted to examine the difference in concentrations predicted by AERMOD and ISCST3. Long et al. (2004) analyzed the concentrations predicted by the two models for point and volume sources in an urban environment and found that AERMOD predicted significantly lower 3, 8 and 24 hour concentrations than ISCST3. Long found that concentrations predicted by AERMOD were twice as sensitive to surface roughness as to solar radiation. Hanna et al. (2000) compared measured concentrations downwind from a ground level area source to AERMOD estimates and reported that AERMOD predicted concentrations 2.5 times the measured values. The pollutant release was non-buoyant and the terrain was an open grassy area with low surface roughness. Faulkner et al. (2007) evaluated the performance of four models ISCST3, AERMOD, Wind Trax and AUSTAL view with measured ammonia concentrations from cattle feed yards and reported that, AERMOD was the only model which predicted higher concentrations of ammonia at night with a

corresponding zero solar radiation relative to concentrations during the day. The other three models predicted lower ammonia concentrations at night similar to what had been observed with measured concentrations. Agricultural sources of air pollution like dairies and cattle feed yards are area sources of PM. These observations suggest that use of AERMOD predicted concentrations for the purpose of regulating 24-hour concentrations off-property from an agricultural source is problematic. The required use of AERMOD for regulatory purposes could lead to inappropriate regulation of the agricultural industry.

Agricultural operations such as harvesting have not been closely regulated in the past. Recently, emissions inventories have included harvesting operations as major contributors to PM emissions in non-attainment areas of California and Arizona (Flocchini et al., 2001). The implications of these inventories coupled with an increased importance to environmental protection have led the SAPRAs in some states to impose stringent limits on PM emissions and requirements for conservation management practices for cotton harvesting in order to reduce emissions. Accurate, science-based emission factors are needed to ensure that appropriate measures are being used for the regulation of these emissions.

An emission factor (EF) is a representative value of the quantity of a pollutant released with an activity associated with the release of the pollutant. (USEPA, 1995) These factors are expressed as the mass of pollutant divided by a unit weight, volume, distance, or duration of the activity emitting the pollutant (e. g., kilograms of particulate emitted per mega gram of coal burned). EFs facilitate estimation of emissions from



various activities. The Emission Factor and Inventory Group (EFIG), in the U. S. Environmental Protection Agency's (EPA) Office of Air Quality Planning and Standards (OAQPS), develops and maintains emission estimating tools to support air quality management decisions. The AP-42 series is the principal means by which the EFIG documents its EFs. The emission factors for cotton harvesting, currently listed in the Environmental Protection Agency (EPA) AP-42 were for PM<sub>7</sub> and were last updated in February 1980 (Wanjura, 2008). Most of the assumptions used in this initial study were based on obsolete harvesting practices. Cotton harvesting practices have changed significantly in the U.S. since 1980.

Flocchini et al. (2001) conducted a study to determine PM<sub>10</sub> EFs from cotton harvesting. The Flocchini study reports PM<sub>10</sub> EFs of 191 kg/km<sup>2</sup> for cotton harvesting using FRM PM<sub>10</sub> samplers and a fixed height box model. Wanjura, (2008) conducted a major field research effort designed to update the cotton harvesting PM emission factors. ISCST3 was used as the model of choice for back-calculating emission rates for two-row and six-row harvesters. This study used the Wanjura data to back-calculate emission factors using AERMOD.

The overall goal of this research was to identify the problems associated with the use of regulatory dispersion models for emissions from agricultural operations and to suggest methods to improve the application of these models. In order to meet this goal, the research addressed these following specific objectives:

1. To develop EFs for PM from cotton harvesting using the Wanjura data but using the AERMOD dispersion model; and to document the differences in EFs as a consequence of models used.
2. To introduce and evaluate a new dispersion modeling approach for field operations like harvesting.
3. To compare downwind concentrations predicted by AERMOD and ISCST3 for PM emissions from ground level areas sources and identify the relationship between the two models.
4. To evaluate AERMOD and ISCST3 predicted concentrations with measured PM concentrations downwind from a cattle feed yard in high plains of Texas.

## CHAPTER II

### EMISSION FACTORS FOR COTTON HARVESTING: A NEW APPROACH TO DISPERSION MODELING FOR HARVESTING OPERATIONS

#### Introduction

Cotton harvesting operations in states like California and Arizona are subjected to increased regulatory pressure from SAPRAs due to regional non-attainment status. Inaccurate emission factors have led to the identification of harvesting as a major contributor to PM<sub>10</sub> emissions in non-attainment areas. Flocchini et al. (2001) reported EFs for PM<sub>10</sub> of 191 kg/km<sup>2</sup> from cotton harvesting for two- to five-row equipment. The protocol used in the study included measuring PM<sub>10</sub> concentrations using Federal Reference Method (FRM) PM<sub>10</sub> samplers and using the concentration data in combination with a mass balance box model to estimate the EFs. The FRM PM<sub>10</sub> samplers have been shown to exhibit significant over-sampling biases when used in the presence of dust with mass median diameter (MMD) greater than 10µm (Buser et al., 2007). The Buser study indicated that the FRM PM<sub>10</sub> sampler could magnify PM<sub>10</sub> concentrations by as much as 340% when sampling a dust with an MMD of 20µm and geometric standard deviation (GSD) of 2.0. The average particle size distribution for emissions from cotton harvesting has an MMD of around 16µm (Wanjura et al., 2006). This induces significant uncertainty to the EFs developed by Flocchini.

Flocchini et al. (2001) used a box model in order to determine the EFs from cotton harvesting. The model (figure 1) consists of a theoretical box with a fixed height of 4 m, placed around the field being sampled. The width of the box was same as the width of the downwind edge of the field. Concentration measurements were made at the upwind and downwind edges of the field using FRM PM<sub>10</sub> samplers. The researchers assumed that there was no reaction of PM inside the box. Therefore, the change in concentration between the upwind and downwind edge of the field was entirely attributed to the sources within the box. The net concentrations (difference between downwind and upwind concentrations) along with wind speeds were used to determine the net mass of PM<sub>10</sub> emitted during the sampling period. The net mass was divided by the area harvested during the sampling period to determine flux. Emission flux was converted to an emission factor by suitable unit conversions (Goodrich, 2006).

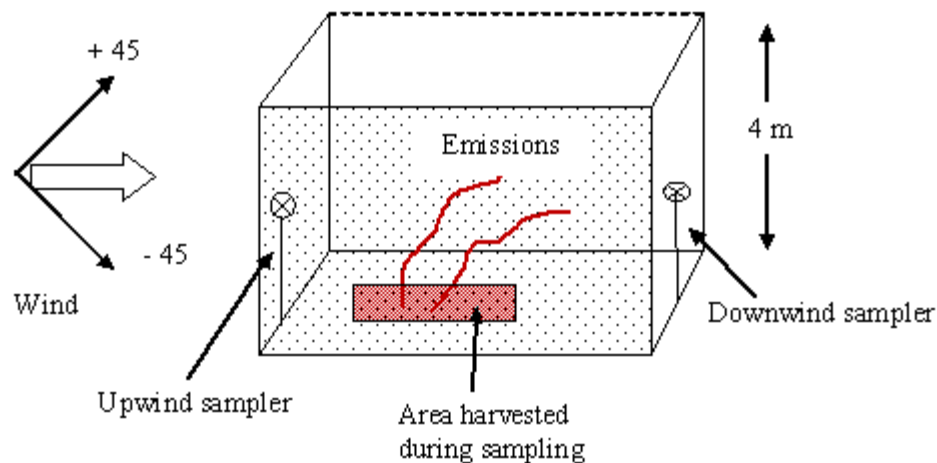


**Figure 1. Schematic of the Flocchini box model**

Goodrich, (2006) provided the following equation (equation 1) to represent the emission flux calculation from the box model.

$$Q = W_B \times H \times C \times U \cos (\theta) \times (1/A) \quad (1)$$

where,

Q = Emission flux,  $\mu\text{g}/\text{m}^2\text{-s}$ ;

$W_B$  = width of the box, m;

H = height of the box, 4 m;

U = wind speed, m/s;

$\theta$  = deviation of wind direction;

C = net concentration,  $\mu\text{g}/\text{m}^3$ ; and

A = area harvested during the sampling period,  $\text{m}^2$ .

Goodrich, (2006) analyzed the application of the box model for developing EFs for agricultural operations and identified the following limitations:

- The model is only valid when the wind direction is  $\pm 45$  degrees from the sampling axis.
- The model is applicable to rectangular area sources only.
- The fixed box height may lead to underestimation of the total emissions, as the plume behavior of large sources cannot be adequately described by a constant mixing height.

Faulkner et al. (2007) and Lange, (2008) found that emission rates by back-calculated using a dispersion model are model specific. This means that if these box model emission rates were used with other dispersion models such as AERMOD or ISCST3, the results would be incorrect estimates of downwind concentrations. Most SAPRAs are using AERMOD to regulate industrial and agricultural sources of air pollution today. Wanjura, (2008) used measured concentrations of TSP and PM<sub>10</sub> with inverse dispersion modeling to back-calculate EFs for two-row and six-row pickers. Wanjura reported PM<sub>10</sub> EFs using ISCST3 at 66 kg/km<sup>2</sup> for six-row picker and 312 kg/km<sup>2</sup> for two-row pickers.

## Methodology

**Ambient Air Sampling for Cotton Harvesting:** The concentration data and meteorological observations for this study were obtained from Wanjura, (2008). The researchers in the Wanjura study conducted collocated TSP and FRM PM<sub>10</sub> concentration measurements for emissions from a two-row and six-row pickers. The sampling was conducted at a farm located 13 km southwest of college station, TX. Figure 2 shows the farm which was subdivided into 21 test plots. Test plots 1-6 had a six-row picker operating and test plots 15-21 had a two-row picker operating. Data for the particle size distribution analysis were also obtained from Wanjura, (2008).

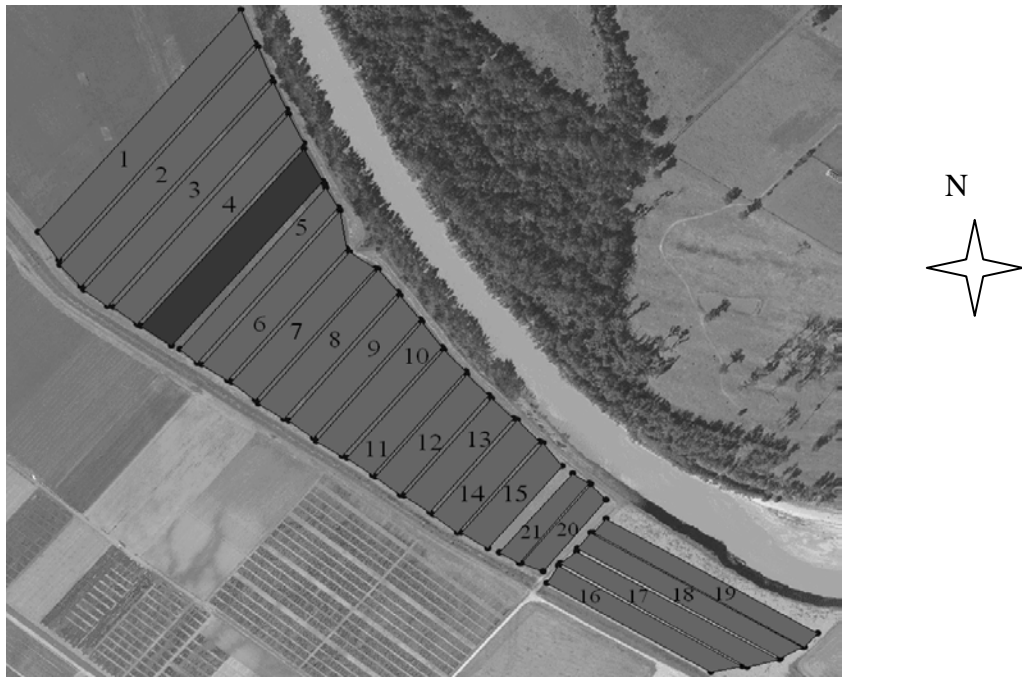


**Figure 2. Layout of test plots**

Emission factor development: The following methodology was used to calculate EFs:

1. Model setup parameters and processed meteorological data were used in the AERMOD dispersion model using a unit emission flux ( $1 \mu\text{g}/\text{m}^2\text{-s}$ ). The model-user interface used for AERMOD was BREEZE AERMOD 6 (BREEZE AERMOD v. 6.2.2, Trinity Consultants, Dallas, TX). The interface used for ISCST3 was BREEZE ISC GIS Pro (BREEZE ISC GIS Pro v. 5.2.1, Trinity Consultants, Dallas, TX)
2. The output of dispersion modeling is a unit flux concentration (UFC) for each test at each sampling location. Dividing the concentration measured in the field at each location by the UFC at that location yields the actual flux at the location. The emission flux ( $\mu\text{g}/\text{m}^2\text{-s}$ ) thus obtained was converted into an EFs by multiplying the sampling time as shown in equation 3.

$$\text{Flux}_{\text{actual}} = C_{\text{measured}} / \text{UFC} \quad (2)$$

$$\text{EF} = \text{Flux}_{\text{actual}} \times C \times \text{ST} \quad (3)$$

where,

UFC = Unit flux Concentration,  $\mu\text{g}/\text{m}^3$ ;

$C_{\text{measured}}$  = Measured concentration,  $\mu\text{g}/\text{m}^3$ ;

$\text{Flux}_{\text{actual}}$  = Pollutant flux from harvest operation,  $\mu\text{g}/\text{m}^2\text{-s}$ ;

C = units conversion factor (0.06);

ST = Sampling time in minutes; and

EF = Emission factor,  $\text{kg}/\text{km}^2$ .

3. The TSP EFs were multiplied by percentage of PM less than  $10 \mu\text{m}$  and  $2.5 \mu\text{m}$  obtained from PSD analysis to get true  $\text{PM}_{10}$  and  $\text{PM}_{2.5}$  EFs, respectively.

EFs for agricultural operations such as dairies, cattle feed yards etc. are typically developed through back-calculating emission fluxes using a dispersion model and simultaneously collected concentration and meteorological data (Goodrich, 2006; Wanjura et al., 2004). In this dispersion modeling approach, emissions were modeled as area sources. This is a reasonable estimate of the existing conditions in feedlots, dairies etc. The alternate hypothesis in this research was to treat harvesting as a mobile source instead of an area source. In such a case, concentrations recorded at the receptors vary with the position of the mobile source. When the harvester moves through the plot, the receptors start capturing PM. The PM collected varied with the position of the harvester. The EFs obtained by treating the harvesting as a mobile source were compared to the



EFs obtained from the area source approximation. The EFs obtained from the area source approximation (Method 1) and the mobile source approximation (Method 2), were correlated with data taken during the Wanjura study (yield, soil moisture etc.) to investigate the trends observed in the EFs.

The protocol for measuring, modeling, and calculating emission factors for fugitive emissions has been established by researchers at Texas A&M (Wanjura et al., 2004). This protocol has been used for area sources with PM emissions. Samplers are deployed around the area to measure PM concentrations emitted from the area source. Samplers on the upwind side of the area source are used to measure the ambient (upwind) concentrations which are subtracted from the downwind concentrations to determine the net PM emitted from the area source. This protocol, referred to herein as “Method 1”, has been used to develop EFs for fugitive area sources. Method 1 was used to determine the emission factors for cotton harvesting. The procedure used consisted of dividing the cotton field into 21 individual strips, or plots (figure 2). Each plot was modeled separately as an area source using an emission flux of  $1 \mu\text{g}/\text{m}^2\text{-s}$  for the duration of the harvest time (T). Receptors in the model corresponding to the actual samplers around the plot. (figure 3).

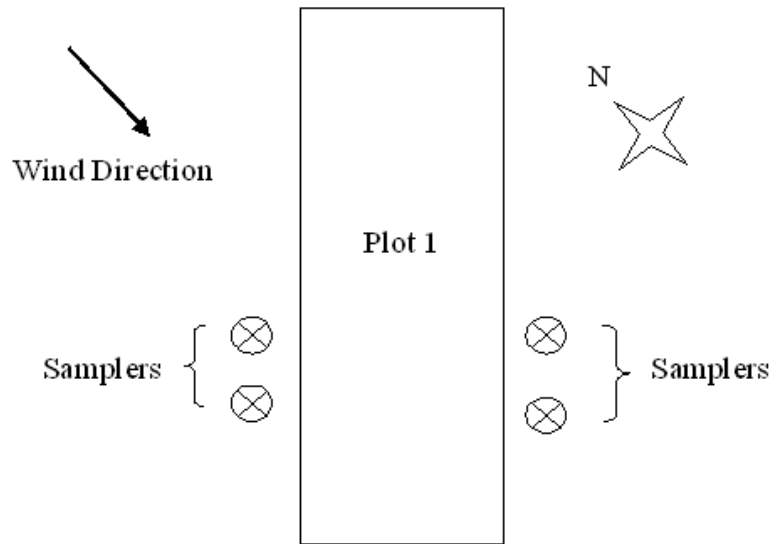


**Figure 3. Method 1 setup in AERMOD**

The meteorological data obtained from the Wanjura study were processed with a five minute averaging time for modeling. A detailed description of this procedure is provided in Appendix B. With an emission flux of  $1 \mu\text{g}/\text{m}^2\text{-s}$ , each plot was modeled using AERMOD to calculate PM concentrations for the model receptors. The PM concentrations measured in the field were divided by the resulting model predicted concentrations as shown in equation 2 to determine the emission flux. Equation 3 was used to convert the emission flux into an emission factor. The same procedure was repeated for each of the plots to develop an EF for each plot. Standard deviations were calculated for the EFs obtained (equation 4). The EFs larger than three standard deviations were treated as outliers and deleted from the analysis.

$$\sigma = \{ \sum [(x_i - \mu)^2 / N] \}^{1/2} \quad (4)$$

where,

$\sigma$  is the standard deviation of the EFs;

$x_i$  is the individual EF;

$\mu$  is the mean EF; and

$N$  is the total number of EFs.

Method 1 has generally been used for area sources like feedlots and dairies. It is assumed that the cattle or dairy animals uniformly stir up PM by hoof action throughout the yard. Field harvesting operations present a different situation where the PM emissions vary during the harvest. The harvester moving through the field entrains PM in strips until the plot has been harvested. Method 2 was developed to address this difference.

Each plot within the field was divided into several line sources, each with a length equal to the total length of the plot and a width equal to the width of the harvester. The number of line sources in each plot was equal to the number of passes taken by the harvester in that plot (Wanjura, 2008). In the model, each line source was given a unit emission flux of  $1 \mu\text{g}/\text{m}^2\text{-s}$ . In the field, when harvester is moving in a single pass PM is emitted only from that pass and the rest of field has zero emissions. To simulate this scenario the line sources were modeled sequentially. For example, consider figure 4 in which the plot contains 6 lines sources. When line 1 is given an input flux of  $1 \mu\text{g}/\text{m}^2\text{-s}$  the remaining four lines 2,3,4,5 have zero emissions. Similarly when line 2 is given an input flux the remaining lines 1,3,4,5 have zero emissions.

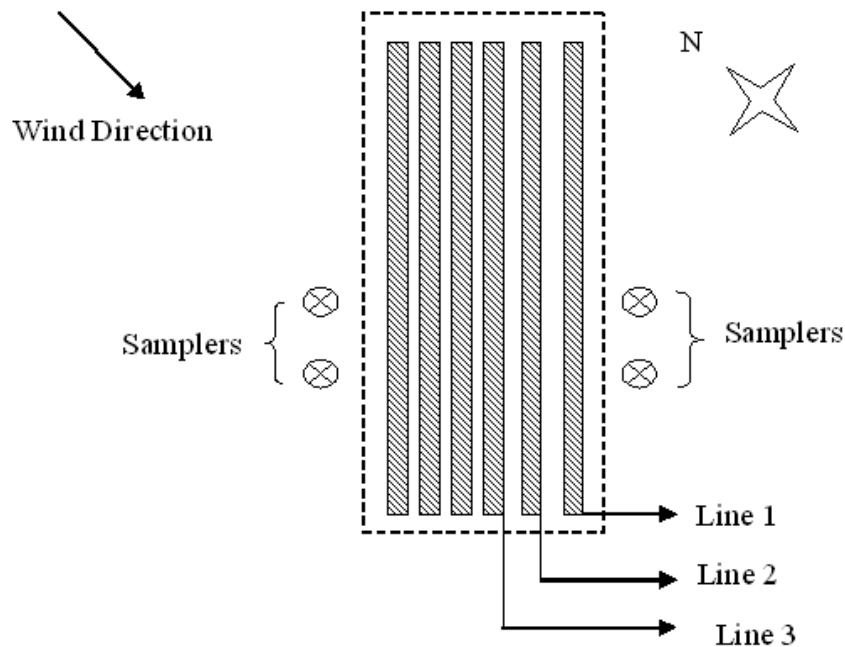


**Figure 4. Method 2 setup in AERMOD**

With Method 2, each successive line source was modeled and concentrations were predicted at all receptors. The modeled concentrations at the samplers were calculated by summing the predicted concentrations due to all the line sources (figure 4). Equation 2 was used to determine the emission flux by dividing the measured field PM concentrations by the corresponding modeled concentrations. Equation 3 was used to calculate the emission factor. The same procedure was repeated for each of the plots to develop an emission factor for the entire field.

The following are the key aspects of modeling common to both Methods 1 and 2:

- Meteorological (met.) data were recorded in the Wanjura study at every quarter of a second. These data were processed to obtain 5-minute average met. data corresponding to the 5 minute intervals during harvesting and the corresponding modeling runs for both Methods 1 and 2. The detailed procedures used to obtain emission fluxes are described in Appendix B.
- The following input parameters were specified for each model run:
  - a. Size and orientation of the emission source;
  - b. A unit emission flux ( $1 \mu\text{g}/\text{m}^2\text{-s}$ )
  - c. 5-minute met. data;
  - d. Emission release height (4 m);
  - e. Receptor locations and heights (2 m); and
  - f. Terrain conditions (flat terrain).
- The outputs of each modeling run were estimated concentrations at the receptors using the unit flux. These are referred to as unit flux concentrations (UFC) in this thesis.
- The TSP and FRM  $\text{PM}_{10}$  concentrations measured in the field were divided by the UFC to obtain the TSP and FRM  $\text{PM}_{10}$  emission fluxes, respectively. These emission fluxes were converted to EFs using equation 3.

The following are the key differences between Methods 1 and 2:

In Method 1, the UFC obtained from each 5-minute modeling run at receptors were a consequence of an average PM emission rate from the entire plot area. The met. data used for modeling runs were 5-minute averages of Wanjura's data. The number of

modeling runs were determined by the number of five minute periods required to complete harvesting of the plot. The resulting flux was an average of all 5-minute modeling runs. For example, if the total time of harvesting an area was 2-hours, there would be 24 lines of met. data. Each data line would correspond to a 5-min average. Dispersion modeling runs were used to estimate concentrations at the receptors for each 5-min met. data line. The maximum UFC was the result used to calculate a flux for the plots as described above.

In Method 2, the total plot area was divided into sub-plots (line sources). The number of line sources corresponded to the number of harvester passes used to harvest the plot area. The GPS data taken during the Wanjura study gave a detailed estimate of the path followed by the harvester in the field. For example, if the harvester took 10 passes to cover an area, 10 line sources were laid out in the model. The GPS data also gave the time taken by the harvester to complete each pass. For example, if the harvester took 10 minutes to complete a pass, the met. data corresponding to that 10 were used in the model run. The UFCs in Method 2 were the results PM emissions by the harvester as it operated in each line source. The number of modeling runs for each line source was determined by the time required to harvest that particular line source. The 5-minute met. data used for modeling runs were a function of the location of the harvester in the plot and the time required to harvest the line sources. The modeling resulting consisted of UFCs for each line source. The resulting fluxes were averaged to yield fluxes and emission factors for the plot.

## Results and Discussion

EFs for four species of PM (TSP, FRM PM<sub>10</sub>, True PM<sub>10</sub> and True PM<sub>2.5</sub>) were developed for each treatment (six-row, two-row) and each modeling method. The results for six-row harvester are listed in Table 1. EFs developed using the two modeling methods were found not to be statistically different for all the four species at the 95% confidence level. No difference was observed even in the standard deviation values of the EFs developed using the two methods. The percentage differences in the mean EF were determined using equation 5.

$$\text{Percent difference} = [(EF_{\text{Method 1}} - EF_{\text{Method 2}}) / EF_{\text{Method 1}}] * 100 \quad (5)$$

where,

$EF_{\text{Method 1}}$  is the EF developed using the Method 1; and

$EF_{\text{Method 2}}$  is the EF developed using Method 2.

FRM PM<sub>10</sub> EFs were 60% higher than True PM<sub>10</sub> EFs, indicating an over-sampling bias of the FRM PM<sub>10</sub> samplers when sampling PM with large MMD dust. PM<sub>2.5</sub> EFs determined using both methods were less than 6 kg/km<sup>2</sup>, indicating that cotton harvesting is not a major contributor of PM<sub>2.5</sub> emissions in the San Joaquin valley.

**Table 1. EFs in kg/km<sup>2</sup> for six-row harvester using Method 1 and 2**

		TSP	FRM PM <sub>10</sub>	True PM <sub>10</sub>	True PM <sub>2.5</sub>
Method 1	Mean	568	376	154	5.46
	Std error	76	69	21	0.68
Method 2	Mean	667	443	180	5.94
	Std error	85	79	23	0.76

The resulting emission factors for the two-row harvester are as listed in the table 2. Similar to the six-row EFs, the two-row EFs developed using methods 1 and 2 were not statistically different at the 95% confidence level. EFs for all the four species were higher for the two-row harvester than the six-row harvester. This indicated that the EFs for six-row harvesters were significantly lower than EFs for two-row harvesters. FRM PM<sub>10</sub> EFs were 40% higher than True PM<sub>10</sub> EFs. This indicated that the FRM PM<sub>10</sub> samplers were subject to oversampling bias when used in the presence of PM with MMD greater than the cut-point of 10  $\mu\text{m}$ .

**Table 2. EFs in kg/km<sup>2</sup> for two-row harvester using Method 1 and 2**

		TSP	FRM PM <sub>10</sub>	True PM <sub>10</sub>	True PM <sub>2.5</sub>
Method 1	Mean	1457	675	425	15.4
	Std error	286	85	83	3.03
Method 2	Mean	1380	626	403	14.6
	Std error	291	73	85	3.09



Spearman rank correlation analysis was carried out between the TSP EFs developed using the two methods and the process variable data obtained from Wanjura, (2008). The process variables considered were crop yield, plot area, soil & seed cotton moisture and percentage of soil mass less than 106  $\mu\text{m}$ . The null hypothesis for this test was that there is no actual correlation between the TSP EFs developed and the process variables. The analysis yielded the results listed in Table 3. The table shows the correlation coefficient (R) and significance (p). The correlation coefficients represent the strength of the relationship between variables. R values closer to 1 indicate a strong correlation. Values of p less than 0.05 indicate that the null hypothesis can be rejected indicating that the correlation between the EFs and the process variable is significant at the 95% confidence level.

**Table 3. Correlation analysis of TSP EFs with process variables**

		Yield <sup>[b]</sup> (bales/km <sup>2</sup> )	Area (km <sup>2</sup> )	% Soil mass < 75 $\mu\text{m}$	% Soil mass > 75 $\mu\text{m}$	Seed cotton moisture (%)	Soil moisture (%)
Method 1	R <sup>[a]</sup>	0.550*	-0.005	0.317*	0.098	-0.462*	-0.413*
	p	0.013	0.484	0.039	0.226	0.014	0.029
Method 2	R	0.620*	-0.093	0.382*	0.031	-0.343*	-0.333*
	p	0.022	0.247	0.024	0.410	0.015	0.017

[a] Yield correlations were performed for six-row harvester only

[b] \* Significant at 0.05 level

TSP EFs showed significant correlation with yield, moisture contents of soil and seed cotton and % soil mass < 75  $\mu\text{m}$ . When the harvester processes more plant material per unit time, it is an indication that the yield is higher with a corresponding increase in PM emissions. Increased PM emissions were indicated by the EF correlation with yield. For both methods, the correlation is significant at the 95 percent confidence level. The EFs showed correlations with soil and seed cotton moisture. As the soil moisture increases the emissions due to entrainment of soil PM decreases and this relation is shown by a negative correlation coefficient. As expected, the EFs showed reasonable correlation with percentage of soil mass less than 75  $\mu\text{m}$ . As the percentage of soil less than 75  $\mu\text{m}$  increases, the concentrations of TSP and PM<sub>10</sub> measured by the receptors increases. When EFs were expressed per unit area of harvest, there were no correlations with the area of the plot in all cases. No difference in trends was observed for EFs from Method 1 and Method 2.

The results for Spearman rank correlation analysis conducted for the FRM PM<sub>10</sub> EFs developed using the two methods are listed in table 4.

**Table 4. Correlation analysis of FRM PM<sub>10</sub> EFs with process variables**

		Yield <sup>[b]</sup> (bales/km <sup>2</sup> )	Area (km <sup>2</sup> )	% Soil mass < 75 µm	% Soil mass < 106 µm	Seed cotton moisture	Soil moisture (%)
Method 1	R <sup>[a]</sup>	0.510*	-0.008	0.320*	0.091	-0.426*	-0.323*
	p	0.014	0.412	0.036	0.203	0.018	0.027
Method 2	R	0.580*	-0.090	0.381*	0.027	-0.310*	-0.356*
	p	0.020	0.213	0.020	0.516	0.014	0.020

[a] \* Significant at 0.05 level

[b] Yield correlations were performed for six-row harvester only

The null hypothesis for these tests was that there were no correlations between the FRM PM<sub>10</sub> EFs developed and the process variables. Table 4 shows the correlation coefficients (R) and significances (p). The correlation coefficient represents the strength of the relationship between the two variables.. R values closer to 1 indicate a strong correlation. Values of p less than 0.05 indicate that the null hypothesis can be rejected. This means that the correlation between the EFs and the process variable is significant at the 95% confidence level. Values of p greater than 0.05 indicate that, the null hypothesis cannot be rejected. This means that there is no correlation between the EF and the process variable under consideration.

Similar to the TSP EFs the PM10 EFs showed significant correlation with crop yield and soil moisture. Similar to the TSP EFs, there were no differences observed between PM<sub>10</sub> EFs from Method 1 and Method 2 in the correlation analysis.

Comparisons of AERMOD and ISCST3 EFs were carried out to identify the differences in EFs as a consequence of model used. The True PM<sub>10</sub> EFs obtained from the methods 1 and 2 using AERMOD were compared to the EFs obtained for the same data with ISCST3 model. While modeling with ISCST3 model, only method 1 was used. It was observed that for the six-row harvester, the EFs for AERMOD and ISCST3 were statistically different. The mean AERMOD EFs were 50% higher than the ISCST3 EFs. For the two-row harvester, the AERMOD EFs were not statistically different from the ISCST3 EFs but the mean AERMOD EF was 25% higher than the ISCST3 EF (Table 5). The table contains the mean EF and 95% confidence limits. (Calculated as 1.96 x Std. error)

**Table 5. Comparison of PM<sub>10</sub> EFs in kg/km<sup>2</sup> from AERMOD and ISCST3**

	six- row	two-row
Method 1 (AERMOD)	154 ± 43	425 ± 178
Method 2 (AERMOD)	180 ± 48	403 ± 181
ISCST3	81 ± 16	322 ± 190

In the Wanjura study, EFs for the six-row picker were obtained from a direct measurement of PM concentrations from the harvester. The results obtained from this source-sampling method represent the most accurate estimates of EFs. However sampling studies like these are very expensive to carryout and also require considerable amount of time and labor. To overcome this trouble, dispersion models ISCST3 and

AERMOD were used in this thesis to develop EFs. Comparisons were made between the source-sampling EFs and the EFs developed by the dispersion models. It was observed that there was no statistically significant difference between the ISCST3 EFs and the source sampling EFs. However, AERMOD EFs were three times higher than the source-sampling EFs. Table 6 shows comparisons between the Wanjura EFs and the EFs developed in this thesis.

**Table 6. Comparison of source-sampling EFs and the EFs developed by dispersion models in  $\text{kg}/\text{km}^2$**

Harvester type	Dispersion model	EFs from dispersion models	Source-sampling EFs from Wanjura study
six-row	ISCST3	$81 \pm 16$	$55 \pm 12$
six-row	AERMOD	$154 \pm 43$	

## Conclusions

EFs for TSP,  $\text{PM}_{10}$  and  $\text{PM}_{2.5}$  from cotton harvesting were determined using AERMOD. Modeling results for two different methods were analyzed. Method 1, in which harvesting was modeled as an area source and Method 2, in which harvesting was modeled as a series of line sources. The Method 1 EFs for True  $\text{PM}_{10}$  were  $154 \pm 43$ ,  $425 \pm 178 \text{ kg}/\text{km}^2$  for six-row and two-row harvesters, respectively. The Method 1 EFs for True  $\text{PM}_{2.5}$  were  $5.46 \pm 1.42$ ,  $15.4 \pm 6.46 \text{ kg}/\text{km}^2$  for six-row and two-row harvesters, respectively. The results of this study indicate that EFs developed using Method 1 and Method 2 were not statistically different. Contrary to our hypothesis, the results lead to

the conclusion that modeling method (Method 1 or Method 2) would not cause difference in EFs. This is an important finding and it suggests that the protocol developed at Texas A&M for developing EFs for area sources (Method 1) can be used for harvesting operations. This would save valuable time in the modeling phase of projects aimed at developing EFs.

A comparison was made between AERMOD EFs and the ISCST3 EFs. This comparison observed that, for a six-row harvester, AERMOD EFs were 1.8 times higher than ISCST3 EFs. This leads to the conclusion that EFs developed with dispersion models are model specific. These EFs should be used in conjunction with the same model with which they were developed. If used with a different model, the results would lead to incorrect estimates of downwind concentrations.

FRM  $PM_{10}$  EFs were 50% higher than True  $PM_{10}$  EFs, indicating that the FRM  $PM_{10}$  samplers have an over-sampling bias when sampling larger MMD PM. For both two-row and six-row harvesters, the  $PM_{2.5}$  EFs were less than  $20 \text{ kg/km}^2$ , indicating that the contribution of  $PM_{2.5}$  from cotton harvesting towards emission inventories is very small.

## CHAPTER III

## COMPARISON OF AERMOD AND ISCST3 FOR EMISSIONS FROM A FEEDLOT

## Introduction

Dispersion modeling results are used by SAPRAs to predict the fate and transport of emissions from industrial sources to comply with regulatory requirements. 40 CFR 51 Appendix W ‘*Guideline on Air Quality Models*’ outlines the requirements of air quality models used for regulatory purposes. The EPA preferred regulatory model was changed from ISCST3 to AERMOD in Dec, 2006. The impact of this change is of interest to regulatory agencies and regulated industries. ISCST3 is a Gaussian dispersion model that uses the normal distribution to describe the horizontal and vertical dispersion of pollutants downwind from the source (Wanjura et. al., 2005). AERMOD is also a steady state Gaussian dispersion model, but differs from ISCST3 in the way the meteorological data is treated. EPA (2004) states that the major improvement in AERMOD over ISCST3 is found in the incorporation of state-of-the-art relationships for flow over complex terrain and in the ability to characterize the planetary boundary layer (PBL) under both stable and convective conditions. The Gaussian dispersion equation for a point source, which is the basis for both models, is as shown below (Cooper and Alley, 2002):

$$C(x, y, z) = \frac{Q}{2\pi u \sigma_y \sigma_z} \exp\left(-\frac{1}{2} \frac{y^2}{\sigma_y^2}\right) \left\{ \exp\left(-\frac{1}{2} \frac{(z-H)^2}{\sigma_z^2}\right) + \exp\left(-\frac{1}{2} \frac{(z+H)^2}{\sigma_z^2}\right) \right\} \quad (6)$$

where,

$C(x, y, z)$  = time average steady state concentration at a point  $(x, y, z)$  ( $\mu\text{g}/\text{m}^3$ );

$Q$  = emission rate ( $\mu\text{g}/\text{s}$ );

$u$  = average wind speed at stack height (m/s);

$y$  = horizontal distance from plume centerline (m);

$z$  = height of receptor with respect to ground (m);

$H$  = effective stack height ( $H=h+\Delta h$ , where  $h$  = physical stack height and  $\Delta h$  = plume rise) (m); and

$\sigma_y, \sigma_z$  = horizontal and vertical plume dispersion coefficients, (m).

In ISCST3, the plume spread parameters,  $\sigma_y$  and  $\sigma_z$ , are expressed as functions of distance from the source of emissions. Martin (1976) published equations that relate the spread parameters to downwind distance ( $x$ ).

$$\sigma_y = ax^b \quad (7)$$

$$\sigma_z = cx^d + f \quad (8)$$

The constants  $a, b, c, d, f$  in the above equations depend on Pasquill Gifford Stability classes and downwind distance. Stability classes (A-F) are estimated from surface wind speed, solar radiation and cloud cover.

AERMOD does not use the discrete Pasquill-Gifford stability classes. AERMET, the meteorological processor for AERMOD, constructs continuous dispersion curves using micrometeorological variables like Monin-Obukhov length and sensible heat flux. The outputs of AERMET are used in AERMOD to estimate plume spread parameters. Due to differences in the model algorithms, the concentrations predicted by AERMOD



and ISCST3 can be different. AERMOD results are being used by SAPRAs to regulate property line concentrations in many cases with EFs developed using ISCST3. It is important to estimate the impact of the ISCST3 derived emission factors utilized in the estimates of off-property concentrations with AERMOD to prevent inappropriate regulations of agricultural sources.

A number of studies have been carried out to evaluate the performance of AERMOD with field measurements, but majority of them have been done for pollutant releases from elevated stacks with buoyant releases. Perry et al. (2005) evaluated AERMOD and ISCST3 with 17 field databases. The Perry study reported the ratios of modeled to observed SO<sub>2</sub> and SF<sub>6</sub> concentrations and concluded that except for one database in which the concentrations were low and the atmospheric conditions were stable, AERMOD consistently performed better than ISCST3. All the databases included in this study were for emissions from a point source. Hanna et al. (2000) examined the performance of AERMOD against near surface releases from area sources and reported that AERMOD had difficulty simulating the dispersion. In this study, the source was located in an open grassy area with flat terrain. The calculated geometric mean ratio of AERMOD to measured concentration was 2.47 according to Hanna et al. (2000). Faulkner et al. (2007) evaluated the performance of four models ISCST3, AERMOD, Wind Trax and AUSTAL view with measured ammonia concentrations from cattle feed yards in rural flat terrain and reported that, AERMOD is the only model which predicted higher concentrations of ammonia during the night time conditions (zero solar radiation) than during the day time. The other three models predicted lower ammonia

concentrations during the night time conditions. The measured data also demonstrated that the concentrations of ammonia during the day were higher than during night time conditions. In a sensitivity analysis study done on ground level area sources, Faulkner et al. (2008) reported that concentrations predicted by AERMOD were found to be highly sensitive to changes in surface roughness and wind speed but not sensitive to changes in solar radiation. This is a point of concern as solar radiation effects the atmospheric turbulence, stability and thereby the downwind concentrations of pollutants. Taking into account the studies conducted on AERMOD, it seems to suggest that AERMOD has a difficulty simulating the night time dispersion of pollutants from area sources.

The objectives of this chapter are:

- Evaluate the differences in concentrations predicted by AERMOD and ISCST3 for PM emissions from ground level area sources.
- Obtain a relationship between concentrations predicted by the AERMOD and ISCST3 models under different meteorological conditions.
- Compare the performance of both models to measured PM<sub>10</sub> concentrations downwind from a cattle feed yard.

## Methodology

### *Hypothetical Source*

A hypothetical cattle feed yard with a PM<sub>10</sub> emission factor of 6.8 kilograms per 1000 head per day (kg/1000 hd-day (15 lb/1000 hd-day) was used as the source of PM

emissions in both models. The feed yard dimensions were 1000 m x 1000 m, located in flat terrain, resembling a feedlot in the high plains of Texas. The cattle spacing was 13.9 m<sup>2</sup>/hd (150 ft<sup>2</sup>/hd) and the ground level PM<sub>10</sub> emission flux was 5.65 µg/m<sup>2</sup>-s which was the PM<sub>10</sub> emission rate from the source. Meteorological data for a single year (1988) was obtained for Deaf Smith County in Texas from the TCEQ database for both models (TCEQ, 2007). The data were modified such that the wind direction was constantly blowing from the area source to the receptor grid in order to maximize the opportunity to observe the differences in both models. A receptor grid of 1000 m x 1000 m with a spacing of 100 m in horizontal and lateral directions was placed directly downwind from the source, starting from the edge of the feed yard. The ISCST3 model has only one meteorological file while AERMOD has two files, one surface file and one profile file. The surface files in AERMOD were modified to obtain two different surface files, one each for a surface roughness of 0.1 m and 1 m to be comparable to rural and urban categories in ISCST3. 1-hour concentrations at 2 m height were used to compare the models.

Four major criteria, atmospheric stability, solar radiation, wind speed, and surface roughness were used to evaluate the performance of the models under different cases. For stability, Monin–Obukhov length was used to classify the atmosphere into 3 sub-categories as: (these classifications are the same used by AERMOD):

- i. Stable:  $L > 0$
- ii. Convective:  $L < 0$
- iii. Neutral:  $L > 500 \text{ m}$  and  $< -300\text{m}$

Three different categories of solar radiation were used:

- i. Solar radiation = zero corresponding to night time conditions.
- ii. Solar radiation  $< 800 \text{ W/m}^2$  corresponding to mornings and evenings.
- iii. Solar radiation  $> 800 \text{ W/m}^2$  corresponding to mid-day.

Wind speed categories were arbitrarily selected starting from 2 m/s with an even increment of 2 m/s, and 12 m/s being the upper limit.

In AERMOD, a specific value can be entered for surface roughness, where as in ISCST3 only a rural or urban option is available. A surface roughness value of 0.1 m is used to compare the rural case in ISCST3 and a value of 1 m was used to compare to urban case.

The model setup parameters and source receptor configuration are shown in figure 5.

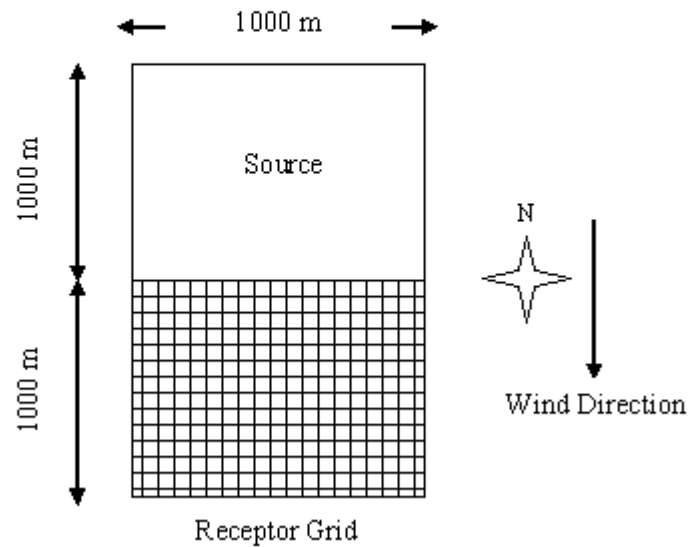


**Figure 5. Model setup parameters**

Percent differences, defined as in equation 8 were used as measures of the differences in the models.

$$\text{Percent difference} = \left[ \frac{(A_{c,i} - I_{c,i})}{I_{c,i}} \times 100 \right] \quad (9)$$

where,

$A_{c,i}$  = AERMOD predicted concentration at  $i^{\text{th}}$  receptor; and

$I_{c,i}$  = AERMOD predicted concentration at  $i^{\text{th}}$  receptor.

*Measured PM Concentrations at a Feedlot*

The PM<sub>10</sub> concentrations and meteorological data used in this research were measurements taken at Feedlot E located in the Texas panhandle during April, 2008 (B. Auvermann, 2008). Feedlot E is a medium size feedlot with 30,000 head of cattle at any one time. R&P Series 1400a Tapered Element Oscillating Microbalance (TEOM) PM<sub>10</sub> downwind concentrations from the feedlot results were used. The TEOM is a Federal Equivalence Method (FEM) sampler. Figure 6 shows the layout of the feedlot with a TEOM sampler 50 m downwind from the north edge of the feedlot. The TEOM recorded concentrations every minute. For the purpose of modeling, the concentrations were converted to a one-hour time averaged concentrations. This resulted in total of 720 1-hour concentrations.

A weather station setup at the north edge of the feedlot recorded all the meteorological data required for ISCST3. But the net solar radiation data were missing. For processing in AERMOD, the missing meteorological variables were assumed the same as those obtained from TCEQ guidance for Deaf Smith County, TX. (Appendix C contains the meteorological data recorded and processed for modeling) The Gaussian distribution which is the basis for both models was originally found to be a good approximation for concentrations over a 10-min averaging time. However, the ISCST3 model used by most SAPRAs uses the 10-min concentrations to approximate 1-hour average concentrations. To assess the performance of the models from a regulatory perspective, 1-hour averaging time was used in this study. An EF of 6.80 kg/1000 hd-day (15 lb/1000 hd-day) was used for the emission factor from the feedlot. (Parnell,

1994) From the available dimensions of the feedlot and number of head (30,000 cattle), the emission flux was calculated as  $6.34 \mu\text{g}/\text{m}^2\text{-s}$ . The atmospheric stability criteria used to evaluate the models were the same as used for the hypothetical feedlot.

This analysis is limited by the fact that PM emission rate from a fugitive source like feedlot is not constant throughout the 24-hr period. The emission rate is dependent upon factors like cattle activity, movement of feed vehicles on unpaved roads etc. However from the data available, an estimate of 24-hr EF (15 lb/1000 hd-day) was selected in this study to compare the model performance with measured concentrations (Parnell, 1994).

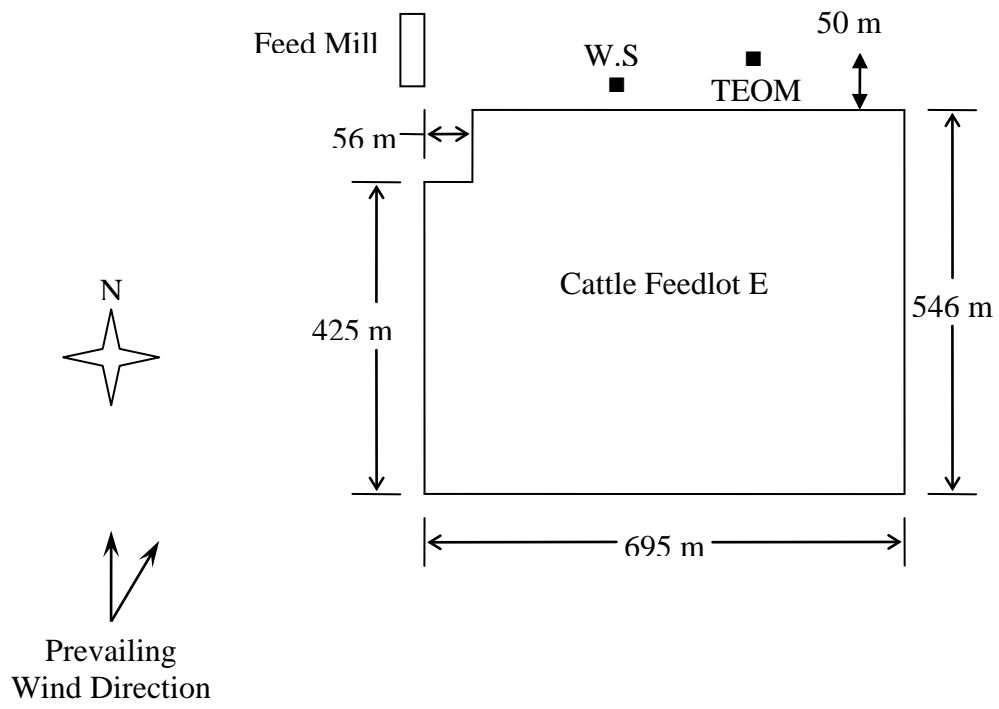
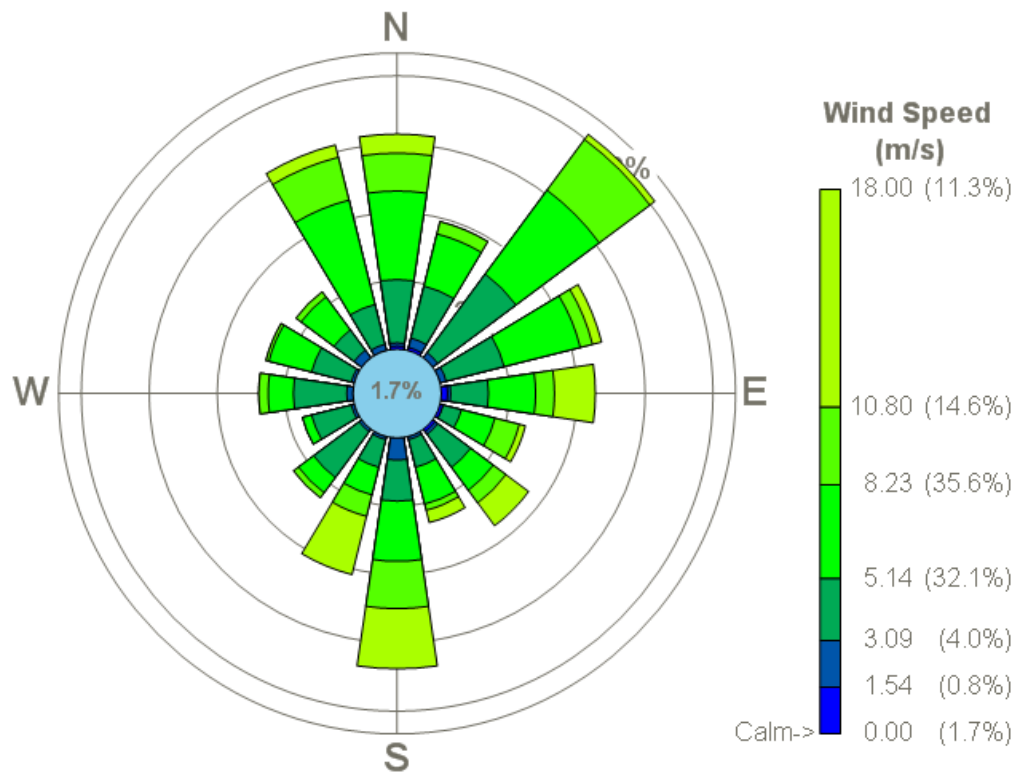


Figure 6. Cattle feedlot with a TEOM sampler



The wind rose diagram (figure 7) shows the distribution of wind speed and direction recorded at the weather station located on the northern edge of the feedlot E (The wind rose shown here depicts the direction towards which wind is blowing).



**Figure 7. Wind rose for feedlot E**

**Statistical Tests:** The two statistical performance measures used to evaluate the performance of AERMOD and ISCST3 were as follows: (1) Normalized mean square error and (2) Fractional bias.

Normalized mean square error (NMSE) was used to estimate the overall deviations between the observed and predicted values. Smaller values of NMSE indicate a better

performance. NMSE does not give indications of over- or under-prediction, but is a measure of the scatter in the data set. The expression for calculating NMSE is shown in equation 9 (Kumar et al., 2006).

$$\text{NMSE} = n \times \frac{\sum_{i=1}^n (P_i - O_i)^2}{\left( \left[ \sum_{i=1}^n P_i \right] \times \left[ \sum_{i=1}^n O_i \right] \right)} \quad (10)$$

where,

$P_i$  is the value predicted by the model at a receptor  $i$ ;

$O_i$  is the measured concentration at receptor  $i$ ; and

$n$  is total number of data points.

Fractional bias normalizes the model bias ( $P_i - O_i$ ) to make it dimensionless. The ranges for FB are +2 to -2. A positive value of FB indicates over-prediction and negative value indicates under-prediction. FB is calculated using equation 10 (Kumar et al., 2006).

$$\text{FB} = 2 \times \frac{\left( \left[ \sum_{i=1}^n P_i \right] - \left[ \sum_{i=1}^n O_i \right] \right)}{\left( \left[ \sum_{i=1}^n P_i \right] + \left[ \sum_{i=1}^n O_i \right] \right)} \quad (11)$$

An ideal model would have an FB and NMSE values of zero. Kumar et al. (2006) report that the 95% confidence intervals on the NMSE and FB values for dispersion models are closer to unity. Thus, to determine the acceptability of a model the following criteria have been set by Kumar et al. (2006).

The performance statistics for the NMSE of the models should be less than 0.5 and the FB should be between -0.5 and 0.5. This would ensure that the concentrations

predicted by the models are within the 95% confidence interval of the observed concentrations.

## Results and Discussion

### *Hypothetical Source*

AERMOD and ISCST3 were used to calculate 1-hr concentrations downwind from a hypothetical ground level area source. Concentrations predicted by the models were compared under different stability and solar radiation ranges. The results shed light on some of the aspects of the performance of these models. A correlation analysis carried out between the percent difference and meteorological inputs to the models yielded the results in table 7. The percent difference between the models were found to be correlated to Monin-Obukhov length and mixing height at the 99% confidence level and correlated to solar radiation at 95% confidence level. Percent difference was not found to be correlated to wind speed.

**Table 7. Correlation analysis**

Correlation	Solar Radiation	Mixing Height	Monin-Obukhov length	Wind Speed
Percent Difference (Rural)	-0.093 <sup>[a]*</sup>	-0.201 <sup>[b]**</sup>	0.129**	-0.052
Percent Difference (Urban)	-0.105*	-0.259**	0.113**	-0.047

[a] \* Significant at 0.05 level

[b] \*\* Significant at 0.01 level

Solar radiation heats the surface of the earth and is the principle cause of turbulence mixing in the atmosphere. Monin-Obukhov length is a parameter that characterizes the relation between different atmospheric mixing phenomena. Thus, both solar radiation and Monin-Obukhov length give an indication of the atmospheric stability. The results shown above (table 7) indicated that differences in the models were due to the way atmospheric stability was handled by the models. A negative sign indicated an inverse relation between solar radiation, mixing height and the percent difference. This implies that during conditions with low mixing height and solar radiation (i.e. during night times), the percent differences in the models were large. The following table (table 8) shows the actual percent differences in concentrations at the edge of the feedlot under different cases.

**Table 8. Percent differences in AERMOD and ISCST3 concentrations at the edge of the feedlot under different atmospheric criteria**

Case	Rural	Urban
Convective	$-29 \pm 1.4^*$	$-7 \pm 1.4$
Stable	$55 \pm 3.3$	$3 \pm 2.4$
Neutral	$-48 \pm 1.3$	$-14 \pm 1.2$
Zero SR	$55 \pm 3$	$11 \pm 3.3$
SR < 800	$-47 \pm 1.2$	$-14 \pm 1.2$
SR > 800	$-46 \pm 1.1$	$-3 \pm 1.3$

\* a negative value indicates AERMOD predicts concentrations lower than ISCST3

For dispersion in a rural surface roughness scenario, the results indicated that AERMOD predicted concentrations significantly lower than ISCST3 for cases when

solar radiation was greater than zero (day time conditions) and when the atmosphere was convective or neutral. These differences range from a minimum of -29% to a maximum of -48%. AERMOD predicted significantly higher concentrations than ISCST3 when there was no solar radiation and when the atmosphere was stable. These differences were 55% for both cases.

For dispersion in an urban surface roughness scenario, the results indicated that AERMOD predicted concentrations lower than ISCST3 for cases when there was solar radiation and when the atmosphere was convective or neutral. These differences ranged from a minimum of -7% to a maximum of -14%. AERMOD predicted higher concentrations than ISCST3 when there was no solar radiation and when the atmosphere was stable. These differences ranged from a minimum of 3% to a maximum of 11%. The percentage differences between the models were significantly lower for the urban cases. The rural surface conditions tended to produce larger differences in the models.

It was hypothesized that the plot of the AERMOD concentrations versus the ISCST3 concentrations would be linear and that a linear regression analysis could be used to develop the relationship between the models. Correlation coefficients ( $R^2$ ) and slopes ( $m$ ) were determined by fitting straight lines without an intercept, between the concentrations predicted by AERMOD and ISCST3.

$$A_{c,i} = m.I_{c,i} \quad (12)$$

where,

$A_{c,i}$  is the concentration predicted by AERMOD at receptor  $i$ ; and

$I_{c,i}$  is the concentration predicted by ISCST3 at receptor  $i$ .

The results of the linear regression analysis between AERMOD and ISCST3 concentrations for different cases at the edge of the feedlot are shown in Tables 9 and 10. Table 9 is for rural surface roughness.

**Table 9. Regression parameters for AERMOD vs. ISCST3 concentrations at the edge of the feedlot for rural surface roughness**

Case	R <sup>2</sup>	Slope	95% C.I Lower	95% C.I Upper	p-value
Convective	0.95	0.40	0.39	0.41	0.00
Stable	0.83	1.69	1.68	1.70	0.00
Neutral	0.99	0.44	0.43	0.45	0.00
Zero solar radiation	0.84	1.76	1.75	1.77	0.00
Solar radiation < 800 W/m <sup>2</sup>	0.90	0.46	0.45	0.47	0.00
Solar radiation > 800 W/m <sup>2</sup>	0.94	0.40	0.39	0.41	0.00

It was observed that the value of R<sup>2</sup> were relatively constant for all cases. The R<sup>2</sup> were less than 0.90 for only two cases: stable and night time conditions. The slopes varied between 0.40 and 1.76. During a stable atmosphere and night time conditions, the slopes were significantly higher for the linear models (1.69 and 1.76). These results indicate that AERMOD predicted concentrations significantly greater than ISCST3 for these scenarios. For the all remaining cases, the slopes were less than 1, indicating that AERMOD predicted concentrations lower than ISCST3. The p-values in the table are used to test the null hypothesis that the corresponding slope is zero. The null hypothesis was rejected for all of the cases because the p-values were not significant at the 0.05

level. The results thus demonstrate that there is a 95% probability that concentrations predicted by AERMOD and ISCST3 can be theoretically approximated by a linear relationship.

Figures 8-13 show the regression plots of AERMOD concentrations versus the property line ISCST3 concentration for the rural surface roughness cases.

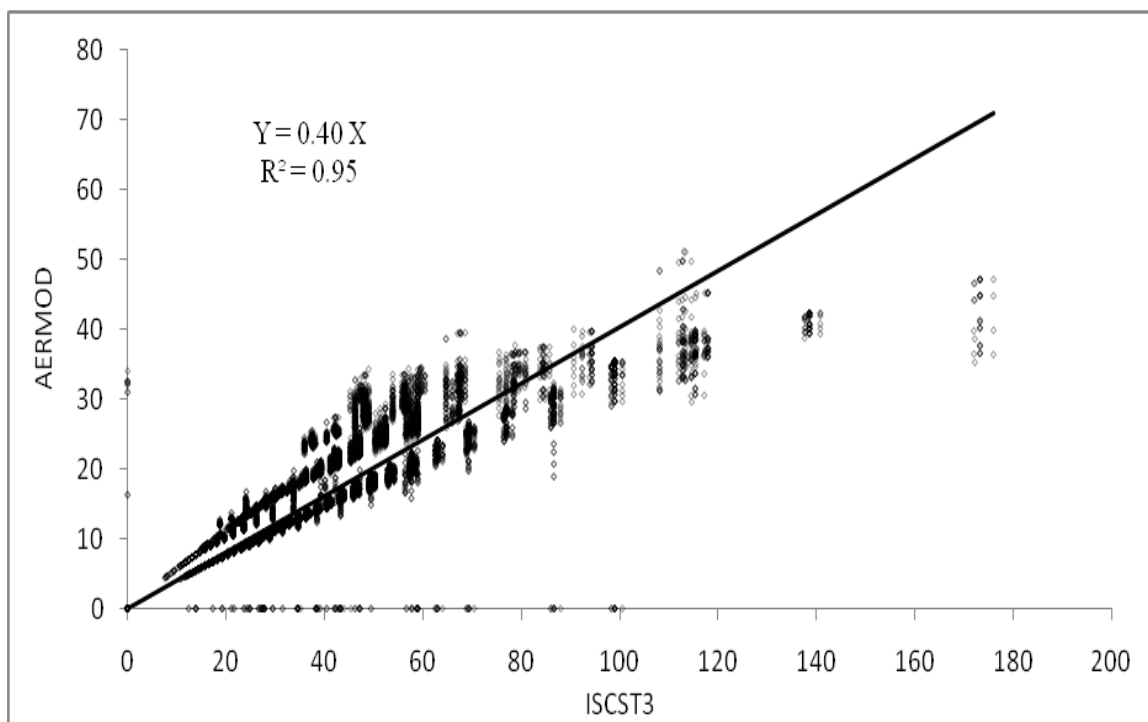


**Figure 8. Regression plot for ISCST3 vs. AERMOD concentrations at the edge of the feedlot in a convective atmosphere**

It can be observed from the figure 8 that in a convective atmosphere AERMOD predicted concentrations approximately 40% of ISCST3. An  $R^2$  value of 0.95 indicated minimum scatter in the data, which is evident from the plot. Deviations from the

regression line can be observed at the lower end of the concentration distribution for concentrations less than  $100 \mu\text{g}/\text{m}^3$ .

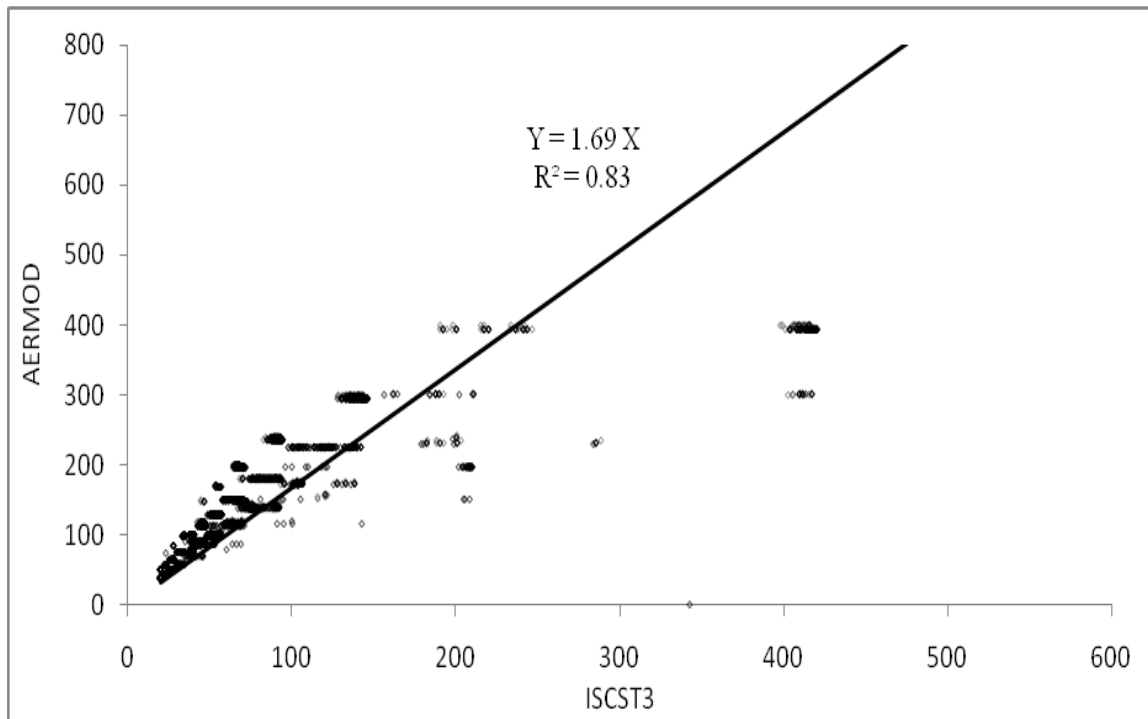


**Figure 9. Regression plot for ISCST3 vs. AERMOD concentrations at the edge of the feedlot in a stable atmosphere**

The regression analysis for the concentrations in a stable atmosphere revealed a marked change from the relationship observed in a convective atmosphere. A slope of 1.69 indicated that AERMOD predicted concentrations 69% higher than ISCST3 in a stable atmosphere. An  $R^2$  value of 0.83 indicated a good fit to the linear model, but deviation from the regression line can be observed at concentrations greater than  $300 \mu\text{g}/\text{m}^3$ . Stable atmospheric conditions are a result of low wind speeds and absence of solar radiation. AERMOD uses the surface heat flux and Monin-Obukhov length instead



of direct solar radiation to determine the plume spread parameters, which is likely the cause for the over-prediction.

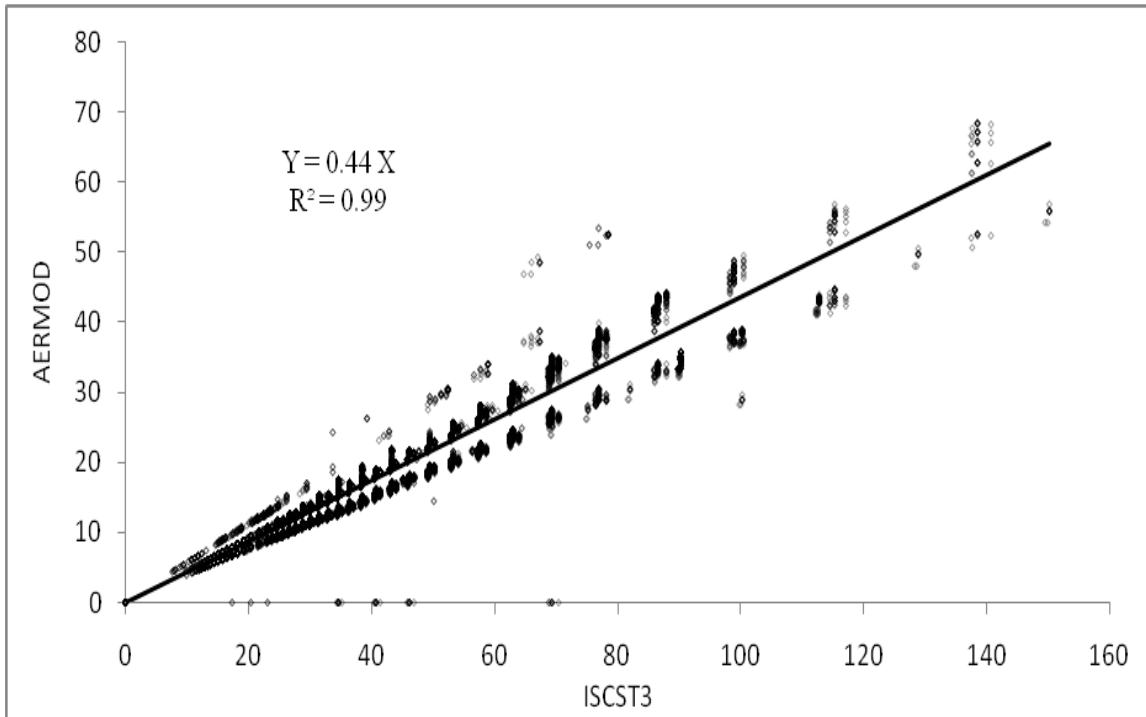


**Figure 10. Regression plot for ISCST3 vs. AERMOD concentrations at the edge of the feedlot in a neutral atmosphere**

In a neutral atmosphere the relationship between the models fits a linear model with an  $R^2$  of 0.99. The deviation of data points from the regression line is very small and occurs at very low concentrations (concentrations less than  $40 \mu\text{g}/\text{m}^3$ ). AERMOD predicted concentrations 44% of ISCST3. The relationship is similar to the relationship observed in a convective atmosphere.

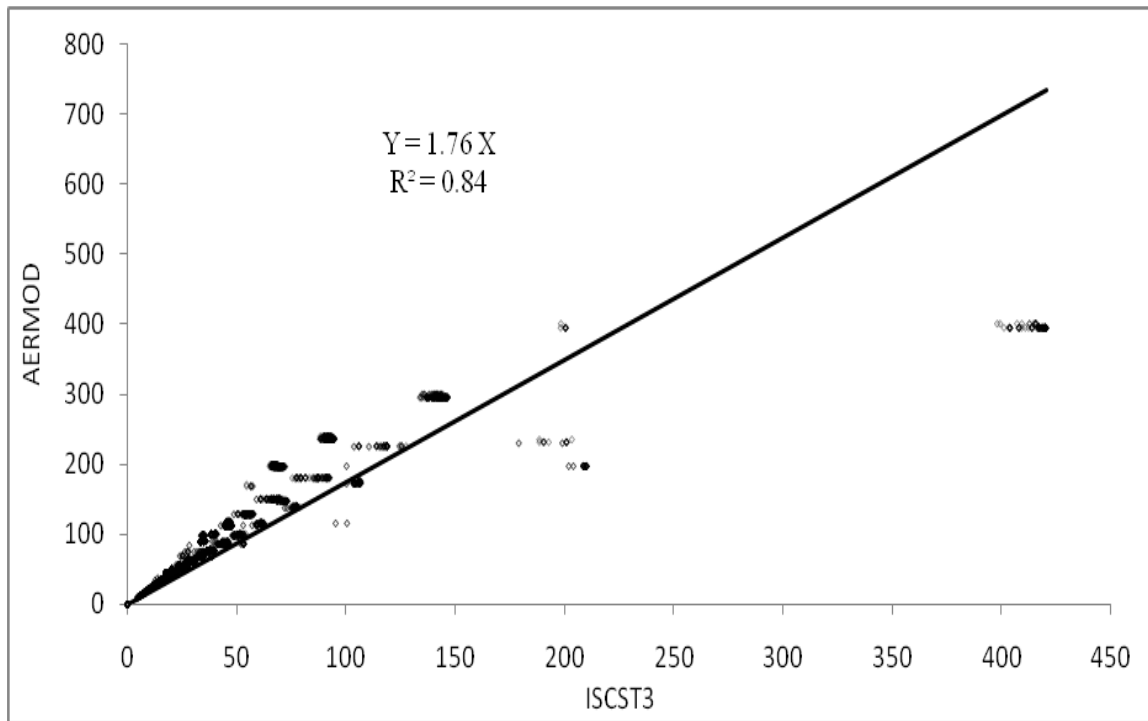


**Figure 11. Regression plot for ISCST3 vs. AERMOD concentrations at the edge of the feedlot when solar radiation is zero**

It can be observed from the figure 11 that in the absence of solar radiation i.e. during the night time, AERMOD predicted concentrations approximately 76% higher than ISCST3.

During the night time due to the absence of solar radiation, the dispersion of pollutants is largely controlled by shear production of turbulence. Interactions between successive layers of air closer to the surface, and terrain features are the primary mechanism for shear production. The result is in agreement with the fact that AERMOD and ISCST3 tend to calculate plume spread parameters differently in such a scenario.

The regression parameters slope and  $R^2$  are similar to those observed in a stable atmosphere (1.69 and 0.83). For concentrations greater than  $400\mu\text{g}/\text{m}^3$ , the relationship deviates from the best fit line and the ratio of AERMOD to ISCST3 approaches one.

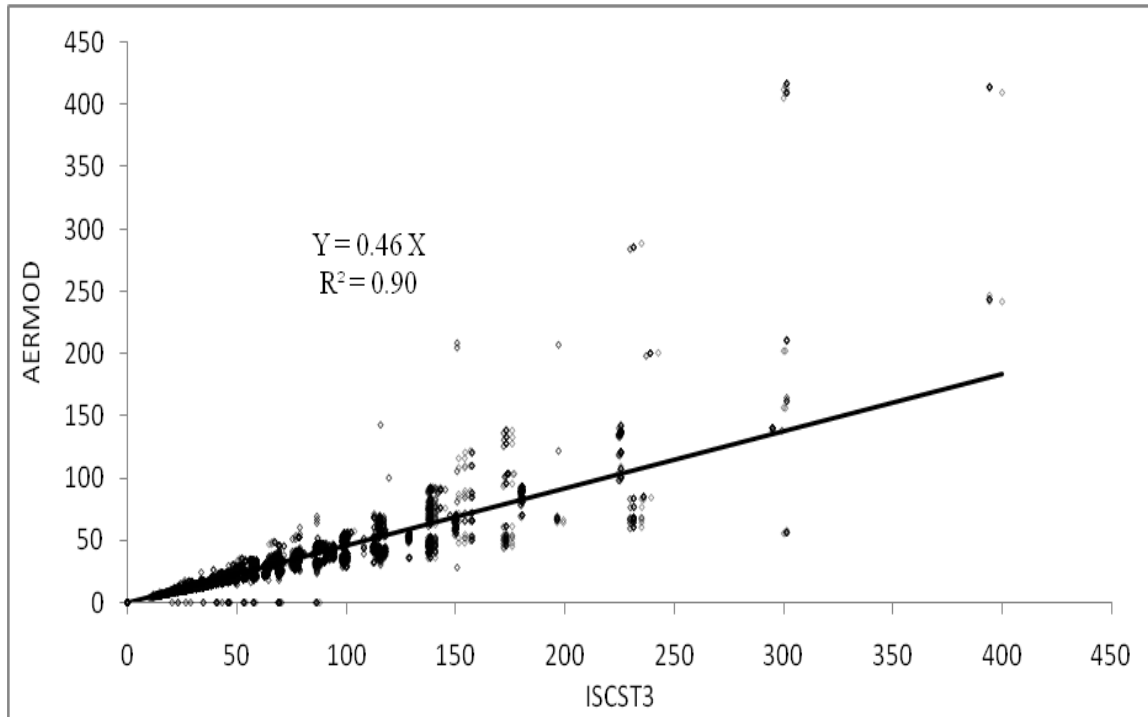


**Figure 12. Regression plot for ISCST3 vs. AERMOD concentrations at the edge of the feedlot when solar radiation  $< 800 \text{ W}/\text{m}^2$**

In presence of solar radiation i.e. during day time, the relationship fits the linear model with an  $R^2$  of 0.90. For both figures 12 and 13, AERMOD predicted concentrations approximately 40% of ISCST3. At concentrations higher than  $300\mu\text{g}/\text{m}^3$ , the ratio of AERMOD to ISCST3 concentrations approaches one. The general trend

observed from different meteorological conditions is that AERMOD predicted concentrations higher than ISCST3 during the night time and lower during the day time.

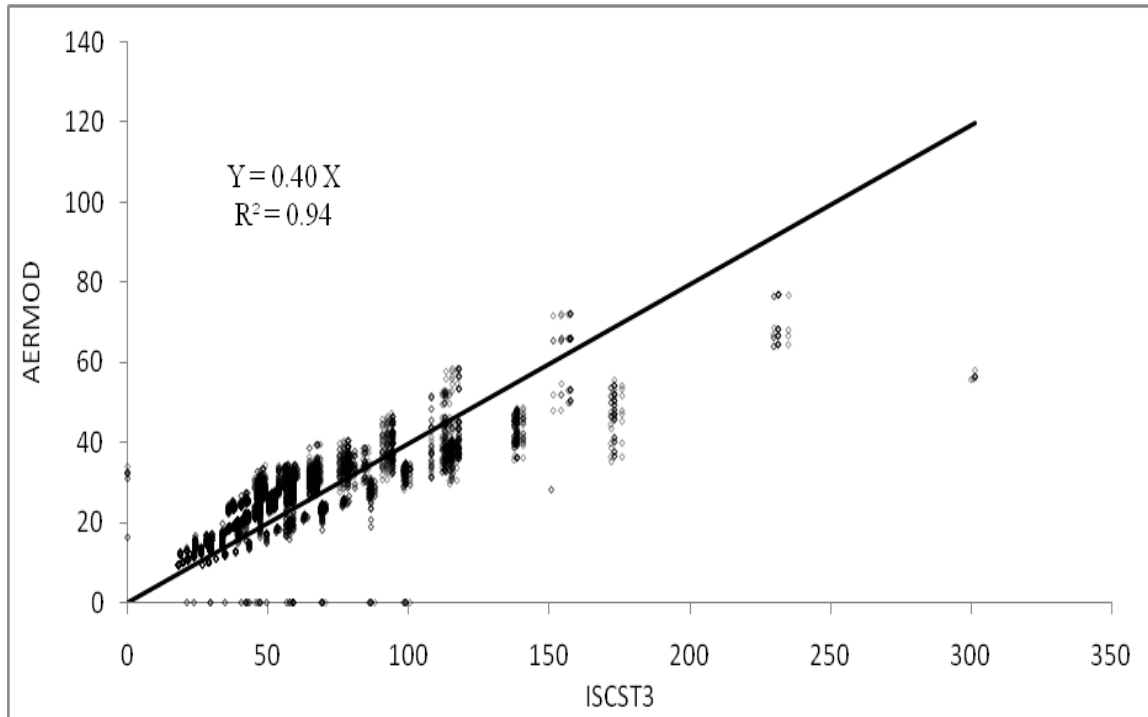


**Figure 13. Regression plot for ISCST3 vs. AERMOD concentrations at the edge of the feedlot when solar radiation  $> 800 \text{ W/m}^2$**

Table 10 shows results of the linear regression analysis for the urban surface roughness scenarios.

**Table 10. Regression parameters for AERMOD vs. ISCST3 concentrations at the edge of the feedlot for urban surface roughness**

Case	R <sup>2</sup>	Slope	95% C.I Lower	95% C.I Upper	p-value
Convective	0.95	0.97	0.96	0.98	0.00
Stable	0.80	1.13	1.12	1.14	0.00
Neutral	0.96	1.08	1.08	1.08	0.00
Zero solar radiation	0.81	1.11	1.10	1.11	0.00
Solar radiation < 800 W/m <sup>2</sup>	0.90	1.11	1.10	1.12	0.00
Solar radiation > 800 W/m <sup>2</sup>	0.96	1.00	1.00	1.00	0.00

It can be observed that the value of R<sup>2</sup> was relatively constant for all cases. The slopes were varying between 0.97 and 1.13. There were fewer differences in the predicted AERMOD and ISCST3 concentrations observed during the day time (solar radiation > 800 W/m<sup>2</sup>). AERMOD concentrations were higher by 13% than ISCST3 concentrations during a stable atmosphere. The slopes of the regression lines were closer to unity in the urban case. This indicated that the difference in the concentrations predicted by the models reduces in an urban surface roughness case. The change in slope during day and night times as in the rural case was absent in the urban case.

The p-values in the table are used to test the null hypothesis that the corresponding slope is zero. The null hypothesis was rejected for all of the cases because the p-values were not significant at the 0.05 level. The results thus demonstrate that there is a 95% probability that concentrations predicted by AERMOD and ISCST3 can be reasonably approximated by a linear relationship.

Figures 14-19 show the regression plots of AERMOD concentrations versus the ISCST3 concentrations at the edge of the feedlot for the urban surface roughness cases.

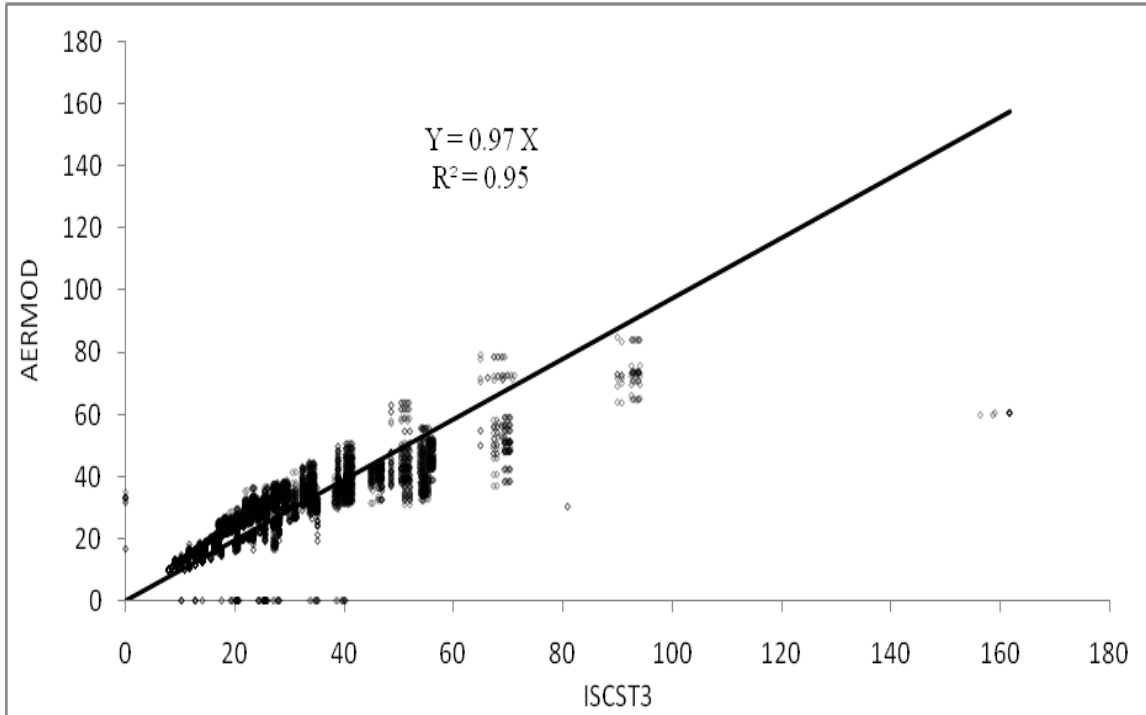


**Figure 14. Regression plot for ISCST3 vs. AERMOD concentrations at the edge of the feedlot in an urban convective atmosphere**

In an urban convective atmosphere, AERMOD and ISCST3 tend to predict similar concentrations. This is indicated by the regression line with a slope of 0.97 and  $R^2$  of 0.95. A convective atmosphere is the result of a strong solar radiation and dispersion in this case is dominated by buoyant turbulence. Both the models tend to produce similar plume spread parameters ( $\sigma_y$  and  $\sigma_x$ ) in such a scenario, resulting in similar concentrations. However, the concentrations predicted by both models in this case are markedly different from a rural convective case. These results suggest that in

addition to meteorological parameters, surface roughness is a major parameter that influences the results using the two models.

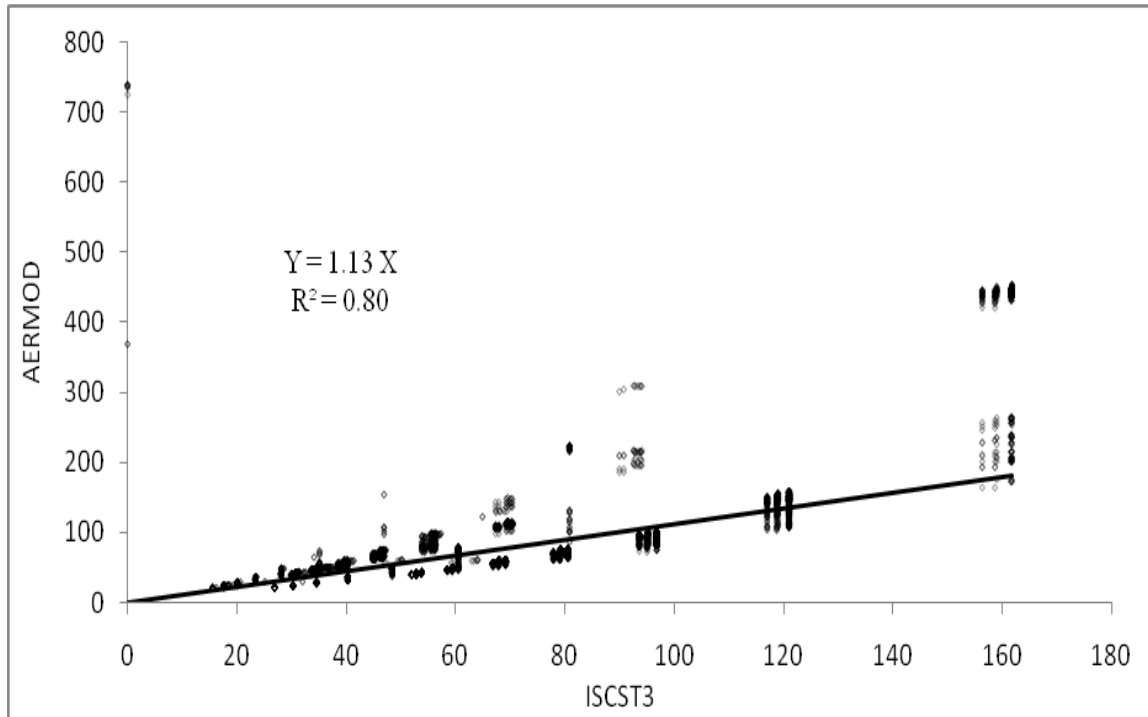


**Figure 15. Regression plot for ISCST3 vs. AERMOD concentrations at the edge of the feedlot in an urban stable atmosphere**

The regression analysis between AERMOD and ISCST3 concentrations in an urban stable atmosphere indicated that AERMOD predicted concentrations 13% higher than ISCST3. The slope of the regression line is lower than the slope for a rural surface roughness (1.76), but the trend of AERMOD predicting higher concentrations than ISCST3 in a stable atmosphere is clear from the figure. At concentrations greater than  $150 \mu\text{g}/\text{m}^3$ , the data points deviate from the regression line. AERMOD predicted concentrations twice as high as ISCST3.

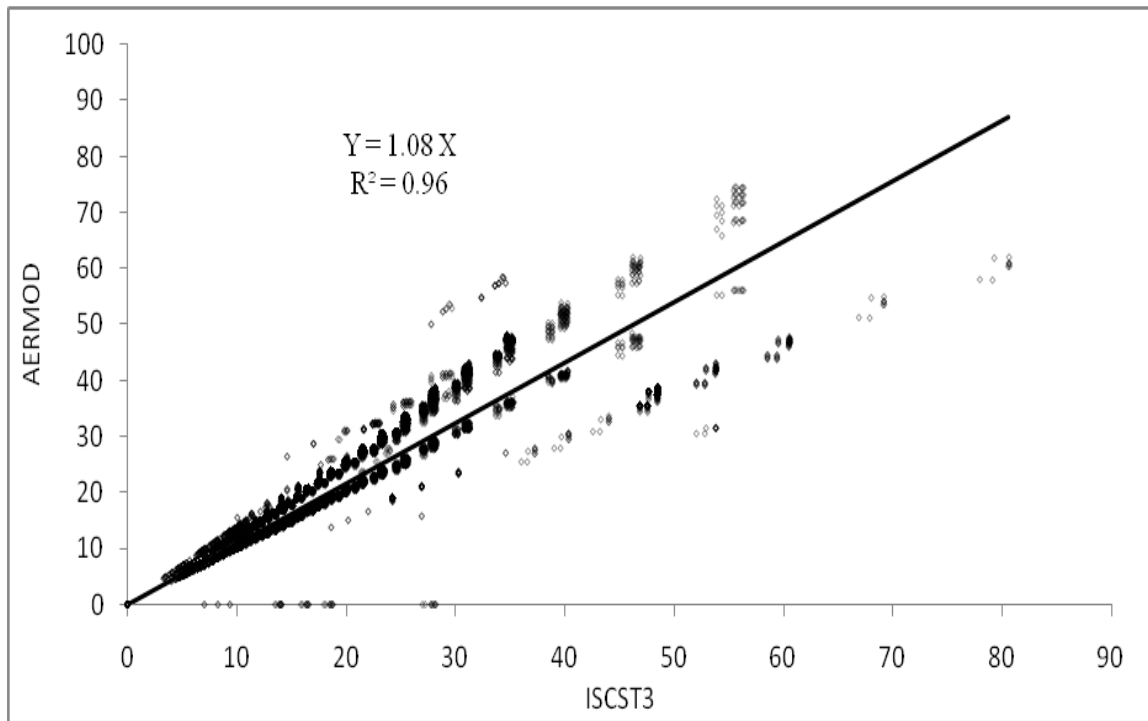


**Figure 16. Regression plot for ISCST3 vs. AERMOD concentrations at the edge of the feedlot in an urban neutral atmosphere**

Regression parameters for a neutral atmosphere, slope of 1.08 and  $R^2$  of 0.96 indicate very little difference for predicted concentrations using the two models. AERMOD predicted 8% higher concentrations than ISCST3. The regression line is similar to that of a convective case (slope of 0.97 and  $R^2$  of 0.95). A neutral atmosphere is a result of moderate solar radiation ( $< 800 \text{ W/m}^2$ ) and wind speeds greater than 5 m/s, when dispersion is dominated by shear production. During this scenario both models tend to produce similar plume parameters ( $\sigma_y$  and  $\sigma_x$ ) resulting in similar concentration outputs.



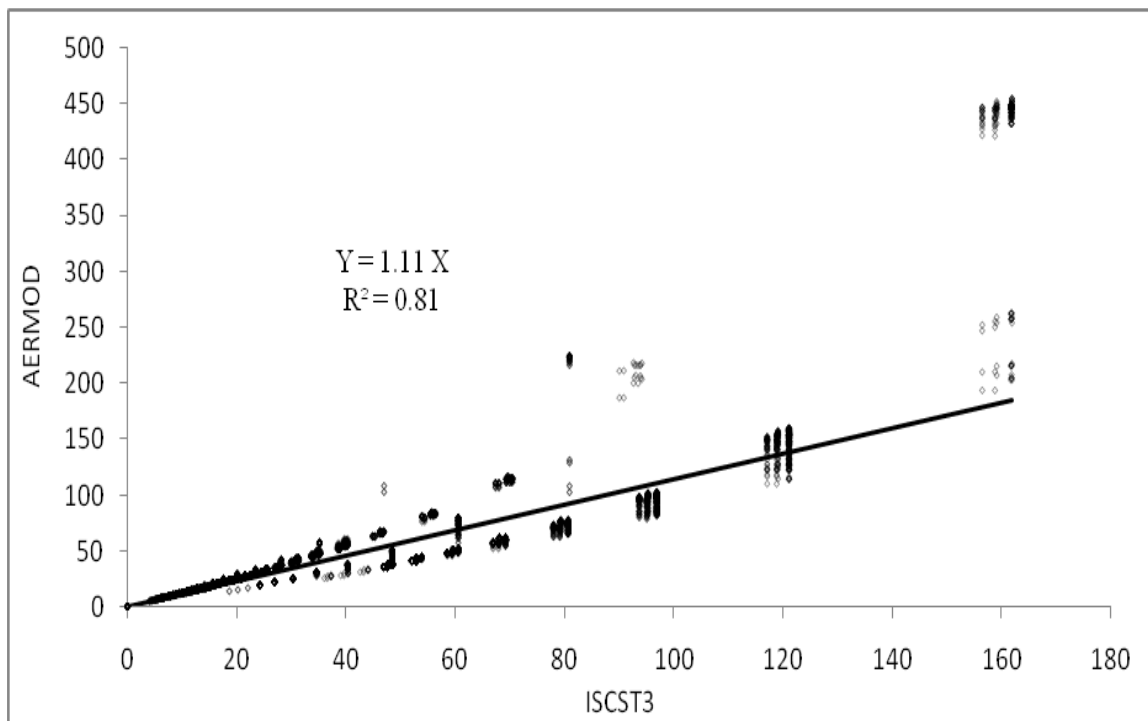


**Figure 17. Regression plot for ISCST3 vs. AERMOD concentrations in an urban case at the edge of the feedlot when solar radiation is zero**

During night time, both the models predict concentrations similar to that in a stable atmosphere. The slope of the regression line is 1.11 which is not different from the slope observed in a stable atmosphere at the 95% confidence level. The ratio of AERMOD to ISCST3 concentrations approaches two at concentrations greater than 150  $\mu\text{g}/\text{m}^3$ . Although the result is in agreement with the trend observed for a rural surface roughness scenario (AERMOD over-predicting during night time), the slope of the line is much lower than that in a rural case (1.76). This suggests that the concentrations predicted by AERMOD and ISCST3 are governed by surface roughness in addition to meteorological conditions.

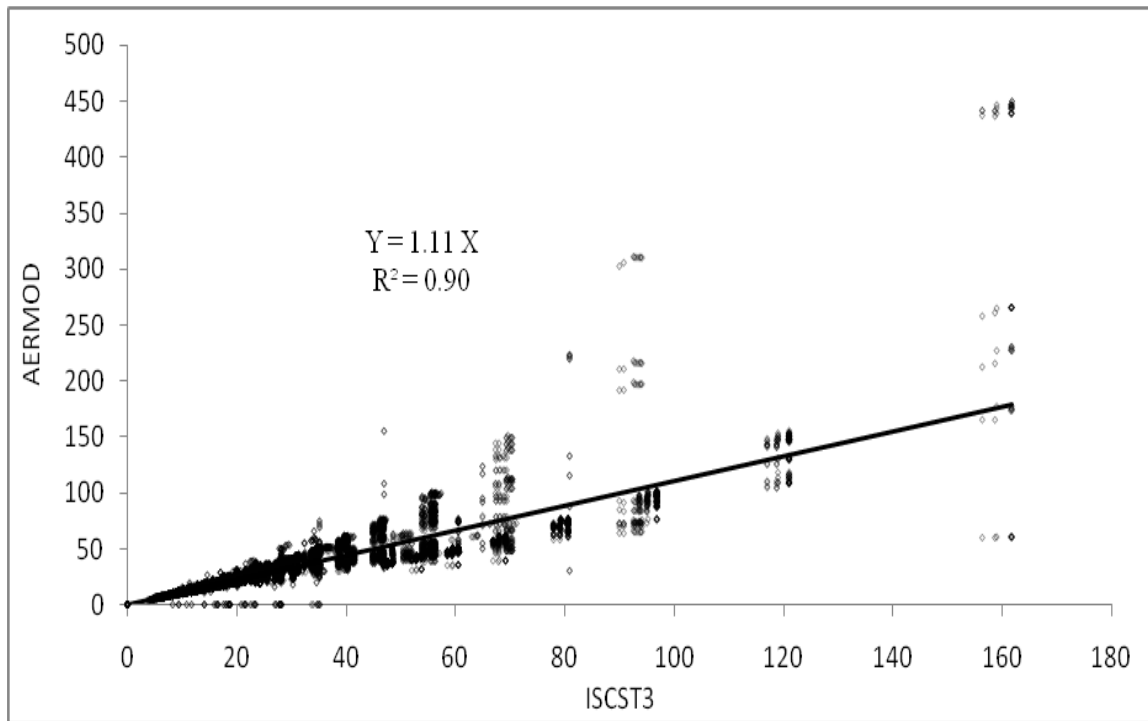


**Figure 18. Regression plot for ISCST3 vs. AERMOD concentrations in an urban case at the edge of the feedlot when solar radiation  $< 800 \text{ W/m}^2$**

The regression analysis for the concentrations in an urban area with solar radiation suggested a marked change from the relationship observed in a rural area. A slope of 1.11 indicated that AERMOD predicted concentrations 11% higher than ISCST3 whereas in a rural area AERMOD under-predicted by 60%. An  $R^2$  value of 0.90 indicated a good fit to the linear model, but deviation from the regression line can be observed at concentrations greater than  $150 \mu\text{g/m}^3$ .

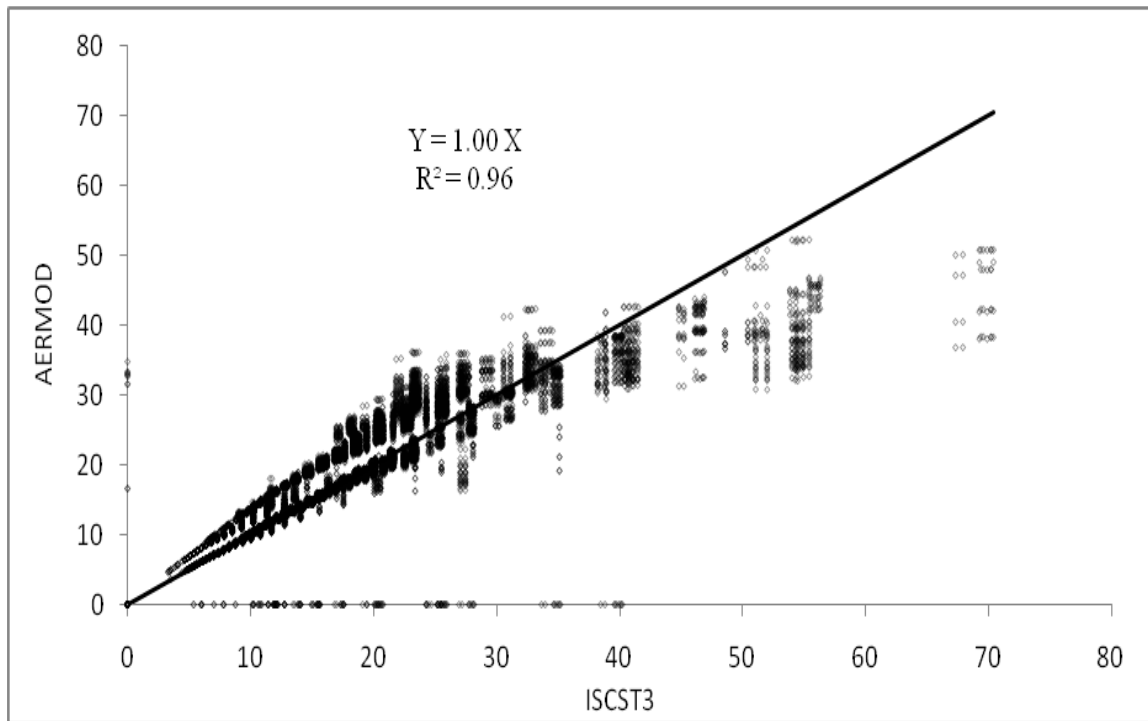


**Figure 19. Regression plot for ISCST3 vs. AERMOD concentrations in an urban case at the edge of the feedlot when solar radiation  $> 800 \text{ W/m}^2$**

A linear regression analysis carried out on the concentrations 500 m downwind yielded the results shown in tables 11 and 12. The null hypothesis tested was that the slope of the regression line was zero. The p-values for all the cases were less than 0.05 implying that the null hypothesis can be rejected.

In a rural Area the slopes of the regression lines varied from 0.19 in a convective case to 2.04 during the night time. During convective and neutral atmospheric conditions, AERMOD predicted concentrations 80% lower than ISCST3. The  $R^2$  values for these cases (0.84, 0.86) indicated a good fit to the linear model. During nighttime and stable atmospheric conditions, AERMOD predicted concentrations twice that of ISCST3. These results are consistent with the trend observed for concentrations at the

edge of the feedlot. However the  $R^2$  values for night time and stable atmospheric cases were lower compared to the remaining cases indicating an increased scatter in the concentration data in the absence of solar radiation.

**Table 11. Regression parameters for AERMOD vs. ISCST3 and rural surface roughness @ 500 m**

Case	$R^2$	Slope	95% C.I Lower	95% C.I Upper	p-value
Convective	0.84	0.19	0.18	0.19	0.00
Stable	0.71	1.94	1.92	1.96	0.00
Neutral	0.86	0.26	0.25	0.27	0.00
Zero solar radiation	0.71	2.04	2.03	2.05	0.00
Solar radiation < 800 W/m <sup>2</sup>	0.72	0.31	0.30	0.32	0.00
Solar radiation > 800 W/m <sup>2</sup>	0.89	0.20	0.20	0.20	0.00

In an urban area, the slopes of the regression lines varied from 0.67 in a convective case to 1.04 in a stable case. During convective and neutral atmospheric conditions, AERMOD predicted concentrations 30% lower than ISCST3. The  $R^2$  values for these cases (0.88, 0.86) indicated a good fit to the linear model. However the  $R^2$  values for night time and stable atmospheric cases were lower (0.64) compared to the remaining cases indicating an increased scatter in the concentration data in the absence of solar radiation. Similar observation was made for the rural area. During nighttime and stable atmospheric conditions, the difference between the models was minimum indicated by a slope approaching one. These results are consistent with the trend observed for concentrations at the edge of the feedlot in an urban area.

**Table 12. Regression parameters for AERMOD vs. ISCST3 and urban surface roughness @ 500 m**

Case	R <sup>2</sup>	Slope	95% C.I Lower	95% C.I Upper	p-value
Convective	0.86	0.67	0.66	0.68	0.00
Stable	0.64	1.04	1.03	1.05	0.00
Neutral	0.88	0.81	0.80	0.82	0.00
Zero solar radiation	0.64	1.00	1.00	1.00	0.00
Solar radiation < 800 W/m <sup>2</sup>	0.90	0.96	0.95	0.97	0.00
Solar radiation > 800 W/m <sup>2</sup>	0.92	0.75	0.74	0.76	0.00

A regression analysis carried out for concentrations at 1000 m downwind gave the results shown in tables 13 and 14.

In a rural area, the slopes of the regression lines varied from 0.15 in a convective case to 2.06 during the night time. The trends observed at the edge of the feedlot and 500 m downwind were repeated at the 1000 m downwind distance i.e. During convective and neutral atmospheric conditions, AERMOD predicted concentrations 80% lower than ISCST3 with a good fit to the linear model (R<sup>2</sup> of 0.83 and 0.95). But, at nighttime and stable atmospheric conditions, AERMOD predicted concentrations twice that of ISCST3. Increased scatter in the concentration data was observed during these periods.

**Table 13. Regression parameters for AERMOD vs. ISCST3 and rural surface roughness @ 1000 m**

Case	R <sup>2</sup>	Slope	95% C.I Lower	95% C.I Upper	p-value
Convective	0.80	0.15	0.14	0.16	0.00
Stable	0.69	1.96	1.94	1.98	0.00
Neutral	0.95	0.23	0.22	0.25	0.00
Zero solar radiation	0.69	2.06	2.04	2.08	0.00
Solar radiation < 800 W/m <sup>2</sup>	0.67	0.29	0.28	0.30	0.00
Solar radiation > 800 W/m <sup>2</sup>	0.86	0.16	0.16	0.16	0.00

In an urban area, similar to the results observed at the edge of the feedlot, AERMOD predicted concentrations 30% lower than ISCST3 in a convective atmosphere. In a stable atmosphere the slope of the regression line was 1.03 indicating a minimum difference between the concentrations predicted by the models.

Overall it can be observed that the relationship between the models remained consistent with downwind distance. The three major factors that characterized the relationship between the models were solar radiation, atmospheric stability and surface roughness.

**Table 14. Regression parameters for AERMOD vs. ISCST3 and urban surface roughness @ 1000 m**

Case	R <sup>2</sup>	Slope	95% C.I Lower	95% C.I Upper	p-value
Convective	0.83	0.61	0.60	0.62	0.00
Stable	0.61	1.03	1.02	1.04	0.00
Neutral	0.85	0.74	0.74	0.74	0.00
Zero solar radiation	0.61	0.61	0.60	0.62	0.00
Solar radiation < 800 W/m <sup>2</sup>	0.66	0.92	0.91	0.93	0.00
Solar radiation > 800 W/m <sup>2</sup>	0.90	0.68	0.67	0.69	0.00

Predicted AERMOD concentrations at the edge of the feedlot were highly variable at wind speeds less than 3 m/s. Figure 20 shows the variance of AERMOD and ISCST3 concentrations at different wind speeds. Variances of concentrations were calculated using equation 12.

$$\sigma^2 = \sum [(C_i - C_\mu)^2] / (n-1) \quad (13)$$

where,

$\sigma^2$  are variances of concentrations,  $(\mu\text{g}/\text{m}^3)^2$ ;

$C_i$  is the concentration predicted by the model in  $\mu\text{g}/\text{m}^3$ ;

$C_\mu$  is the mean concentration predicted by the model for a wind speed category in  $\mu\text{g}/\text{m}^3$ ; and

$n$  is the number of concentrations in the wind speed category.

Lower wind speeds generally occur during late evenings and lead to stable conditions. This is the period when dust peaks have been observed downwind from feedlots (Hamm, 2005). During the dust peak phenomenon concentrations predicted by AERMOD had a very high variance. The variance of ISCST3 concentrations is lower compared to AERMOD concentrations.

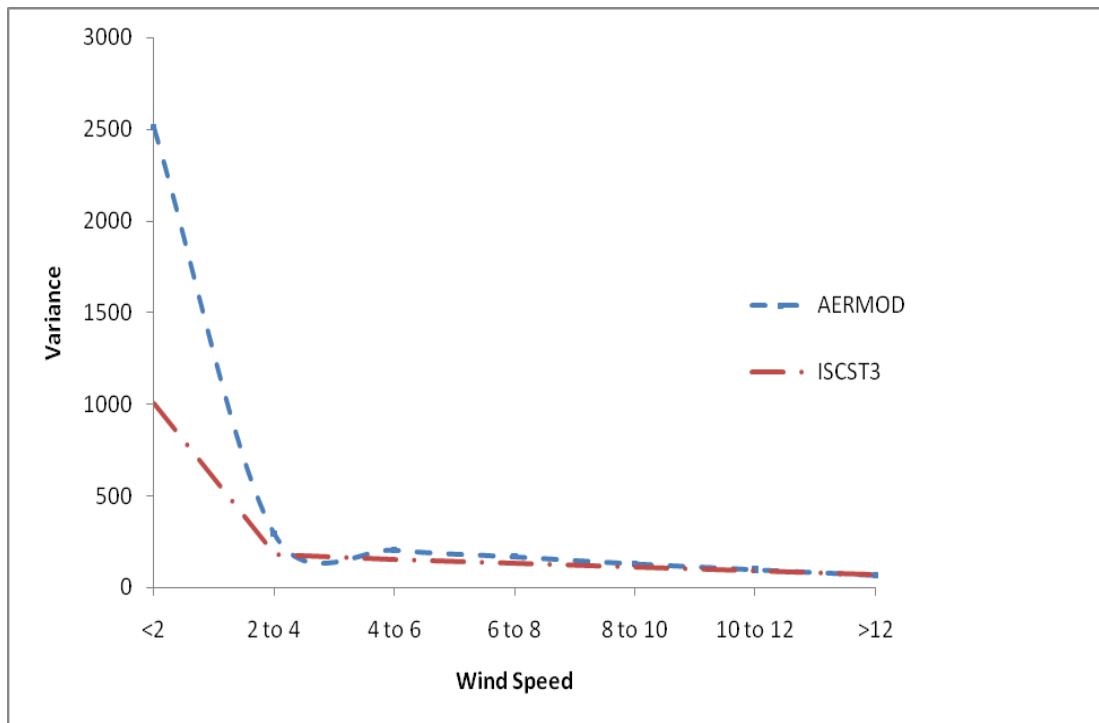


**Figure 20. Variance in AERMOD and ISCST3 concentrations as a function of wind speed**

#### *Measured PM Concentrations at a Feedlot*

The following tables (table 15 and 16) shows the NMSE and FB values for ISCST3 and AERMOD under different cases. It was observed that for all cases the FB values for both models were positive. This means both the models tend to predict concentrations higher than observed values.



**Table 15. NMSE and FB values for AERMOD under different atmospheric criteria**

Model		convective	Stable	Neutral	Zero solar radiation	Solar radiation < 800	Solar radiation > 800
AERMOD	FB	0.38	1.30	0.41	1.24	0.41	0.31
	NMSE	0.49	9.26	0.54	8.74	0.69	0.45
n		331	214	175	251	211	258

**Table 16. NMSE and FB values for ISCST3 under different atmospheric criteria**

Model		convective	Stable	Neutral	Zero solar radiation	Solar radiation < 800	Solar radiation > 800
ISCST3	FB	0.68	0.71	0.98	0.71	0.79	0.62
	NMSE	0.69	0.79	1.48	0.87	0.81	0.72
n		331	214	175	251	211	258

The performance of the models can be termed acceptable for regulatory purposes if the NMSE values are less than 0.5 and the FB values are within the range (-0.5, 0.5) (Kumar et al., 2006).

The results can be summarized for each case as follows:

- **Convective Atmosphere:** It was observed that AERMOD predicted concentrations closer to the measured data than ISCST3. NMSE and FB values of AERMOD were acceptable where as ISCST3 values were not acceptable.
- **Stable Atmosphere:** Both models tended to over-predict concentrations in a stable atmosphere. NMSE and FB values for ISCST3 are around 0.8 indicating that ISCST3 does a better job at predicting concentrations in this case. The corresponding values for AERMOD were too large. The NMSE of 9.26 exceeded the limits for acceptability. This indicated a serious problem with AERMOD estimates of concentrations during stable atmospheric conditions.
- **Neutral Atmosphere:** AERMOD predicted concentrations were closer to the measured field data than ISCST3 concentrations. FB and NMSE values of ISCST3 were not acceptable. FB for AERMOD was within acceptable limits but NMSE for AERMOD exceeded the limits.
- **Zero Solar Radiation:** The performance of the models was similar to a stable atmosphere case. FB and NMSE values for AERMOD exceeded the acceptable limits by a large margin (NMSE of 8.74). Although ISCST3 over-predicted concentrations, this model did a better job than AERMOD. The concentrations were closer to field measurements indicated by the FB value of 0.71.
- **Solar Radiation < 800 W/m<sup>2</sup>:** AERMOD performed better than ISCST3. FB for AERMOD was within acceptable limits but NMSE exceeded the acceptable range. NMSE and FB values for ISCST3 do not fall within the acceptable limits.

- Solar Radiation  $> 800 \text{ W/m}^2$ : NMSE and FB values of AERMOD were within acceptable regions; An FB of 0.31 for AERMOD indicated a high degree of reliability during this case. ISCST3 concentrations were not within required degree of acceptance for this case.

In summary, ISCST3 showed a constant trend for all the cases, with minimum variability in the FB and NMSE values. The performance of ISCST3 model does not vary significantly with atmospheric conditions. AERMOD performed better for the cases when there was a convective or neutral atmosphere. But, the performance of AERMOD during night times and stable conditions is a point of concern. The model tended to significantly over-predict concentrations indicated by large FB values. Unlike ISCST3, the performance of AERMOD varied with atmospheric stability. The results indicated an inconsistency in the model in the absence of solar radiation.

Figures 21 and 22 show the scatter plots of the AERMOD concentrations versus the measured concentration for the two periods, night time (zero solar radiation) and day time with solar radiation less than  $800 \text{ W/m}^2$ . A linear regression analysis was carried out for the concentrations during the night time. However, during the day time, the relationship between AERMOD concentrations and measured concentrations was closer to a step function rather than a linear function. The reason behind this behavior could be the effect of evening dust peaks. During the evenings, the meteorological conditions were characterized by very low wind speeds and stable atmospheric conditions. In such conditions, the PM concentrations downwind from the feedlot could be as high as 2000

$\mu\text{g}/\text{m}^3$ . As the modeled concentrations were directly related to met. data and emission rate, the sudden step function increase was observed.

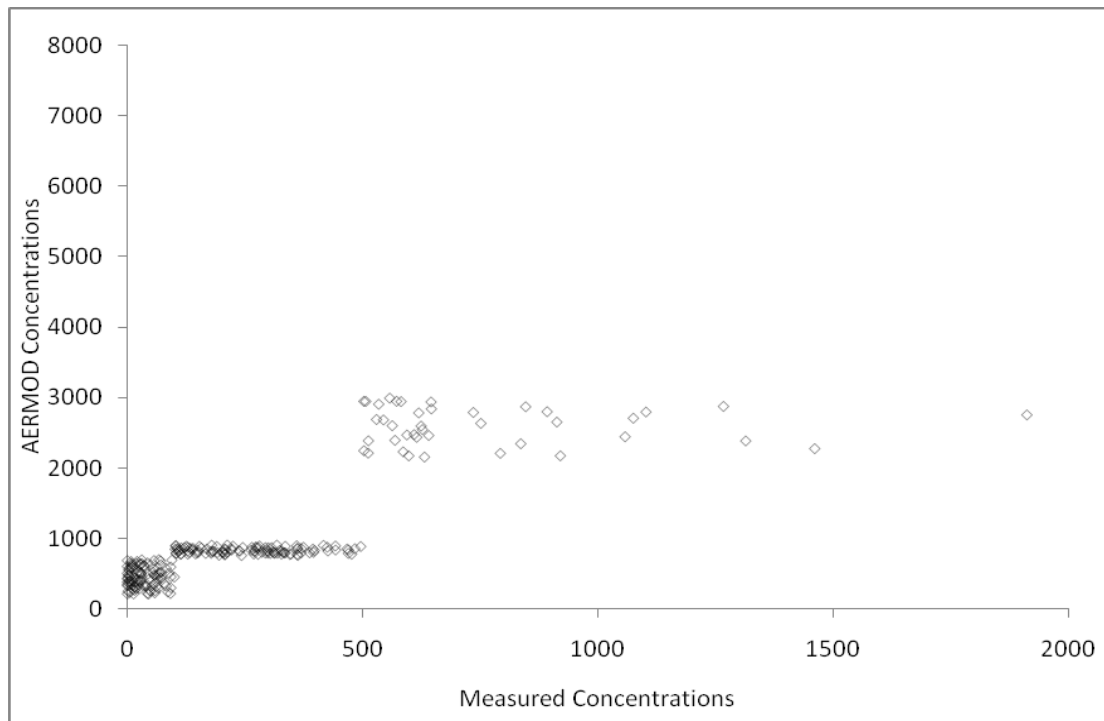


**Figure 21. Scatter plot for measured vs. AERMOD concentrations when solar radiation < 800 W/m<sup>2</sup>**

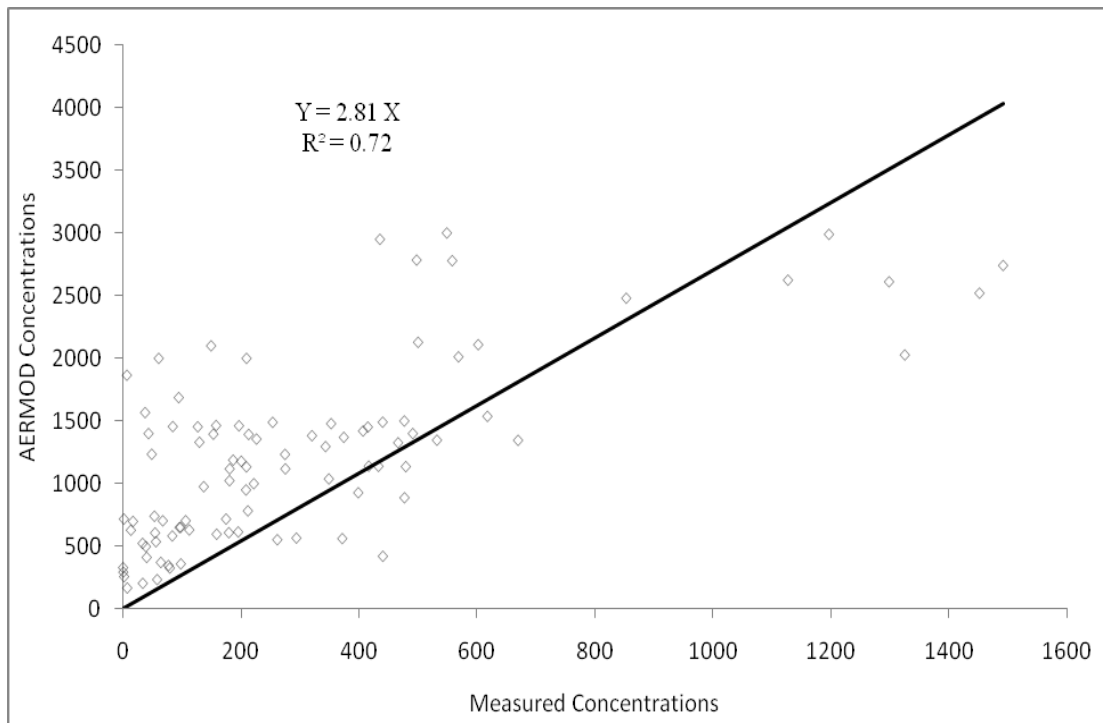


**Figure 22. Regression plot for measured vs. AERMOD concentrations during the night time**

The above plot shows the results of a linear regression analysis between AERMOD and measured concentrations 50 m downwind from a feedlot during the night time. AERMOD predicted concentrations three times higher than the measured values, which is indicated by a slope of 2.81. The  $R^2$  value for the linear model was 0.77 due to scatter in the data. During the night time, there is a positive temperature gradient at the ground surface i.e. thermal radiation emitted from the ground exceeds the radiation from the atmosphere. This inhibits turbulence and thereby the dispersion of pollutants. AERMOD tended to over-predict concentrations in such a scenario.

The following are the results that were obtained from the comparisons between AERMOD and ISCST3 predicted concentrations for the hypothetical source.

- AERMOD predicted concentrations significantly lower than ISCST3 for the following cases:
  - a. 29% lower for a convective atmosphere
  - b. 48% lower for a neutral atmosphere
  - c. 46% lower in presence of in presence of solar radiation  $> 800 \text{ W/m}^2$
- AERMOD predicted significantly higher concentrations than ISCST3 for the following cases:
  - a. 55% higher for a stable atmosphere
  - b. 55% higher in absence of solar radiation (night time)
- Downwind concentrations predicted by AERMOD were highly variable for wind speeds less than 3 m/s.
- The percentage differences between AERMOD and ISCST3 concentrations (1-hour) were significantly higher for a rural surface roughness than for an urban surface roughness.

The following are the results that can be obtained from the evaluation of the models with measured 1-hour field concentrations.

- The performance statistics for AERMOD were within acceptable limits set forth by Kumar et al. (2006) for the following cases:
  - a. Convective atmosphere
  - b. Neutral atmosphere

- c. In presence of solar radiation (day time)
- The performance of AERMOD was not acceptable for the following cases:
  - a. Stable atmosphere
  - b. Absence of solar radiation (night time)
- The performance of AERMOD varied significantly with atmospheric conditions.
- AERMOD predicted concentrations three times higher than the measured values during night times and stable atmospheric conditions. This result demonstrates that solar radiation might not be properly accounted for in the AERMOD dispersion algorithm.

## Conclusions

A linear regression analysis was conducted to determine whether concentrations predicted by AERMOD and ISCST3 were significantly different. Concentrations predicted by the models for a hypothetical feedlot in a rural flat terrain were compared under different stability and solar radiation ranges. The important conclusion drawn from this study was that the impact of solar radiation was different on the concentrations estimated by the two models. During the day time, AERMOD predicts concentrations 40% lower than ISCST3. But, during the night time there is an inverse phenomenon and AERMOD predicts concentrations 60% higher than ISCST3.

The two models were further evaluated with measured PM concentrations at the edge of a feedlot in Texas. The results led to the conclusion that AERMOD is

inconsistent in estimating concentrations for stable atmospheric conditions and during night time. During the night time, AERMOD predicted concentrations three times higher than the measured values. This is a point of concern as AERMOD is the EPA preferred regulatory model. If not addressed this problem might cause significant over-prediction of emissions from ground level sources in rural areas.



## CHAPTER IV

### SUMMARY AND CONCLUSIONS

The air pollution regulatory process is dependent upon accurate estimates of downwind concentrations from sources to protect public health and welfare. The two dispersion models used to perform these predictions have been ISCST3 and the newest preferred model AERMOD. Based on the 24-hr concentrations estimated by these models, SAPRAs determine the compliance of air pollution sources with NAAQS.

An evaluation of AERMOD and ISCST3, with measured PM<sub>10</sub> concentrations from a feedlot in Texas led to the conclusion that AERMOD concentration results are inconsistent when estimating concentrations during night time conditions. In the absence of solar radiation (night time), AERMOD predicted concentrations three times higher than the measured concentrations. This over-prediction problem will likely impact the source's ability to comply with limits set forth by SAPRAs. If this inconsistency is not addressed, it will lead to incorrect estimates of downwind concentrations from rural area sources of PM. In effect, this problem will result in facilities being required to implement more efficient and costly PM controls to achieve compliance with permitted concentration limits off property. Reducing emissions using more efficient and sophisticated abatement strategies increases the economic impact on these facilities. Thus, it is recommended that appropriate correction measures be incorporated in the model algorithm to ensure accuracy in estimated concentrations off property. One

correction approach would be including solar radiation as an input to the model's met. processor and characterizing atmospheric stability as a function of solar radiation.

Cotton harvesting was identified as a major contributor to  $PM_{10}$  emissions in San Joaquin Valley of California. However, limited data were available on PM EFs for cotton harvesting operations. To address this issue, Wanjura, (2008) conducted an exhaustive sampling study to determine the PM concentrations from six-row and two-row cotton pickers. Data collected in this study included meteorological (met.) data for every quarter of a second and GPS data corresponding to the movement of the harvester during testing. Wanjura used the Texas A&M protocol (as described in Chapter II), in conjunction with the ISCST3 model and 20-min averages of met. data to calculate EFs. In this thesis, these Wanjura data were used in conjunction with EPA's current preferred model AERMOD to develop EFs for cotton harvesting. A 5-min averaging time was used to calculate the met. data required by the models. Comparisons of the AERMOD EFs with ISCST3 EFs indicated that AERMOD EFs were 1.8 times higher than ISCST3 EFs. These results suggest that EFs developed using dispersion models are model specific. EFs should be used in conjunction with the same model with which they were developed to ensure accurate estimates of downwind concentrations.

A new approach to model PM emissions from harvesting operations was introduced in this research. This approach included modeling harvesting as a series of line sources, with each line corresponding to a harvester pass in the field. In this approach, we used 5-min averages of met. data and GPS data to better simulate field conditions. It was hypothesized that this more detailed and tedious approach would lead

to improved accuracies of EFs. However, the final results indicated that the more sophisticated approach that better approximated field conditions did not translate to difference in EFs. There were no significant differences between EFs developed by this new approach and the conventional Texas A&M protocol.

The major findings of this work were:

- The AERMOD EFs for  $PM_{10}$  and  $PM_{2.5}$  EFs from a two-row harvester were determined as  $425 \pm 166$  and  $15.4 \pm 6.46$   $kg/km^2$  respectively.
- The AERMOD EFs for  $PM_{10}$  and  $PM_{2.5}$  from a six-row harvester were determined as  $154 \pm 43$ , and  $5.46 \pm 1.42$   $kg/km^2$ , respectively.
- The PM emissions from a six-row picker were significantly lower than emissions from a two-row cotton picker.
- EFs for cotton harvesting developed using dispersion models are model specific and for a six-row picker AERMOD EFs were 1.8 times higher than the ISCST3 EFs.
- There were no significant differences observed between cotton harvesting EFs developed by Texas A&M protocol and the new line source modeling approach described in this research.
- Evaluation of AERMOD and ISCST3 estimated concentrations with measured PM concentrations downwind from a feedlot in Texas indicated that night time results using AERMOD are incorrect for downwind concentrations from area sources.

## REFERENCES

- Auvermann, B. 2008. Unpublished data: PM<sub>10</sub> concentration measurements using TEOM, Amarillo, TX.: Texas AgriLife Research and Extension Center.
- Buser, M. D., C. B. Parnell, Jr., B. W. Shaw, and R. E. Lacey. 2007. Particulate matter sampler errors due to the interaction of particle size and sampler performance characteristics: Ambient PM<sub>10</sub> samplers. *Trans. ASABE* 50 (1): 229-240.
- CFR. 1999. National primary and secondary ambient air quality standards. *Code of Federal Regulations* 40 CFR, Part 50. Washington, D.C.: Office of the Federal Register.
- Cooper, C. D. and F. C. Alley. 2002. *Air Pollution Control: A Design Approach*. 3<sup>rd</sup> ed. Prospect Heights, IL.: Waveland Press Inc.
- Faulkner, W. B., J. J. Powell, J. M. Lange, B. W. Shaw, R. E. Lacey, and C. B. Parnell, Jr. 2007. Comparison of dispersion models for ammonia emissions from a ground-level area source. *Trans. ASABE* 50(6): 2189-2197
- Faulkner, W. B., B. W. Shaw, and R. Grosch. 2008. Sensitivity of two dispersion models AERMOD and ISCST3 to input parameters for a rural ground-level area source. *J. Air and Waste Management* 58: 1288-1296
- Flocchini, R. G., T. A. James, L. L. Ashbaugh, M. S. Brown, O. F. Carvacho, B. A. Holmén, R. T. Matsumura and K. T. Chris. 2001. Sources and sinks of PM<sub>10</sub> in the San Joaquin Valley, final report. USDA – Special Research Grants Program. Contract Nos. 94-33825-0383 and 98-38825-6063. Davis, CA: University of California at Davis.
- Goodrich, L. B. 2006. A PM<sub>10</sub> emission factor for free stall dairies. M.S. thesis. College Station, TX.: Texas A&M University, Department of Biological and Agricultural Engineering.
- Hamm, L. B. 2005. Engineering analysis of fugitive particulate matter emissions from cattle feed yards. M.S. thesis. College Station, TX.: Texas A&M University, Department of Biological and Agricultural Engineering.

- Hanna, S. R., B. A. Egan, J. Purdum, J. Wagler. 2000. Comparison of AERMOD, ISC3, and ADMS model performance with five field data sets. In *Proc. Air and Waste Management Assoc. 2000 Annual Conference*, 1-14, Salt Lake City, UT.: Air and Waste Management Assoc.
- Kumar, A., S. Dixit, C. Varadarajan, A. Vijayan, A. Masuraha. 2006. Evaluation of the AERMOD dispersion model as a function of atmospheric stability for an urban area. *J. Environmental Progress*. 25(2): 141-151.
- Lange, J. M. 2008. Engineering analysis of the air pollution regulatory process impacts on the agricultural industry. M.S. thesis. College Station, TX.: Texas A&M University, Department of Biological and Agricultural Engineering.
- Long, G. E., J. F. Cordova, and S. Tanrikulu. 2004. An analysis of AERMOD sensitivity to input parameters in the San Francisco bay area. In *Proc. 13th Joint Conference on the Applications of Air Pollution Meteorology*, 203-206. Pittsburgh, PA.: The Air & Waste Management Association.
- Martin, D. O. 1976. The change of concentration standard deviation with distance. *J. Air Pollution Control Association* 26 (2):145-146.
- Parnell, S. 1994. Dispersion modeling for prediction of emission factors for cattle feedyards. M.S. thesis. College Station, TX.: Texas A&M University, Department of Biological and Agricultural Engineering.
- Perry, S. G., A. J. Cimorelli, R. J. Paine, R. W. Brode, J. C. Weil, A. Venkatram, R. B. Wilson, R. F. Lee, W. D. Peters. 2005. AERMOD: A dispersion model for industrial source applications. Part 2: Model Performance against 17 Field Study Databases. *J. Appl. Meteorol.* 44: 694-708.
- TCEQ. 2007. AERMET meteorological dataset for Deaf Smith County, TX.: Texas Commission on Environmental Quality. Available at:  
<ftp://ftp.tceq.state.tx.us/pub/OPRR/APD/AERMET/AERMETv06341/AERMETDataSetsByCounty/DeafSmith/>.
- USEPA. 1995. Compilation of air pollutant emission factors AP-42. Research Triangle Park, NC.: Environmental Protection Agency.
- USEPA. 2004. AERMOD: Description of model formulation. EPA-454/R-03-004. Office of Air Quality Planning and Standards – Emissions Monitoring and Analysis Division. Research Triangle Park, NC.: Environmental Protection Agency.

- Wanjura, J. D., C. B. Parnell, Jr., B. W. Shaw and R. E. Lacey. 2004. A protocol for determining a fugitive dust emission factor from a ground level area source. ASAE Paper No. 044018. Ottawa, Ontario, Canada: ASAE.
- Wanjura, J. D., C. B. Parnell, Jr., B. W. Shaw, and R. E. Lacey. 2005. Design and evaluation of a low volume total suspended particulate sampler. *Trans. ASAE* 48(4): 1547-1552.
- Wanjura, J. D., C. B. Parnell, Jr., B. W. Shaw, and S. C. Capareda. 2006. Particle size distribution of PM emitted from cotton harvesting. ASAE Paper No.: 064168. St. Joseph, MI.: ASABE.
- Wanjura, J.D. 2008. A science based emission factor for particulate matter emitted from cotton harvesting. Ph.D. diss. College Station, TX.: Texas A&M University, Department of Biological and Agricultural Engineering.

APPENDIX A  
METEOROLOGICAL DATA FOR MODELING

AERMOD requires the input of two meteorological input files. A surface file and a profile file. The surface meteorological data file consists of the following input variables:

1. Year
2. Month (1 - 12)
3. Day (1 -31)
4. Julian day (1 - 366)
5. Hour (1 - 24)
6. Sensible heat flux ( $\text{W/m}^2$ )
7. Surface friction velocity,  $u^*$  ( $\text{ms}^{-1}$ )
8. Convective velocity scale,  $w^*$  ( $\text{ms}^{-1}$ )
9. Vertical potential temperature gradient in the 500 m layer above the PBL
10. Height of the convectively-generated boundary layer (m)
11. Height of the mechanically-generated boundary layer (m)
12. Monin-Obukhov length,  $L$  (m)
13. Surface roughness length,  $z_0$  (m)
14. Bowen ratio
15. Albedo
16. Wind speed (m/s) used in the computations
17. Wind direction (degrees) corresponding to the wind speed above
18. Height at which the wind above was measured (m)



19. Temperature (K) used in the computations
20. Height at which the temperature above was measured (m)
21. Precipitation code
22. Precipitation rate (mm/hr)
23. Relative humidity
24. Station pressure (milli bars)
25. Cloud cover (tenths)

The contents of the profile meteorological data file are as follows:

1. Year
2. Month (1 - 12)
3. Day (1 -31)
4. Hour (1 - 24)
5. Measurement height (m)
6. Top flag = 1, if this is the last (highest) level for this hour, 0, otherwise
7. Wind direction for the current level (degrees)
8. Wind speed for the current level (m/s)
9. Temperature at the current level (C)
10. Standard deviation of the wind direction,  $F_2$  (degrees)
11. Standard deviation of the vertical wind speed,  $F_w$  (m/s)

ISCST3 contains only one meteorological input file with the following inputs:

1. Year
2. Month
3. Day
4. Hour
5. Flow vector (degrees)
6. Wind speed (m/s)
7. Ambient temperature (K)
8. Stability class
9. Rural mixing height (m)
10. Urban mixing height (m)

APPENDIX B  
METEOROLOGICAL DATA PROCESSING  
FOR COTTON HARVESTING DATA

The weather station in the field recorded the required data for processing and developing meteorological files in AERMOD (Wanjura, 2008). The data was recorded at equal intervals of 0.25 seconds. The primary data recorded includes:

1. Principal orthogonal wind components (measured by 3D anemometer u, v, w)
2. Sonic temperature and relative humidity (T/RH probe mounted in a solar radiation shield at 2m)
3. Barometric pressure (BP sensor)
4. Solar radiation up and down (by 2 pyranometers facing up and down)

The principal orthogonal wind components can be split into a mean component ( $\bar{u}$ ) and a perturbation ( $u'$ ). Temperature is also made up of an average and perturbing component (Van Boxel et al., 2004). Generally the mean component is indicated by an over bar and perturbation by a prime.

$$u = \bar{u} + u' \quad (1)$$

$$v = \bar{v} + v' \quad (2)$$

$$w = \bar{w} + w' \quad (3)$$

$$T = \bar{T} + T' \quad (4)$$

Perturbations in principal wind components u, v and w are used to calculate many input variables for AERMOD. The values recorded by the anemometer should not be directly used in this process as it may lead to errors. The sonic anemometer has fixed vertical coordinates, but the vertical wind direction keeps changing, this is a change in value of w. However it is interpreted as changes in u and v along with w by the anemometer. To

correct for these errors the following methodology (three rotations) as described by Van Boxel et al. (2004) was used

The first rotation (yaw rotation) focuses the u direction of the instrument into the wind direction. It is calculated as follows.

$$\theta = \arctan(\overline{v_m} / \overline{u_m}) \quad (5)$$

$$u_1 = u_m \cos \theta + v_m \sin \theta \quad (6)$$

$$v_1 = -u_m \sin \theta + v_m \cos \theta \quad (7)$$

$$w_1 = w_m \quad (8)$$

where,

$\theta$  = yaw angle in degrees;

$u_m, v_m, w_m$  are components of wind speed measured by sonic anemometer (m/s) and

$u_1, v_1, w_1$  are components after first rotation.

The second rotation (pitch rotation) orients 'u' in the direction of sloping stream lines and 'w' perpendicular to 'u'. It is calculated as shown below.

$$\phi = \arctan(\overline{w_1} / \overline{u_1}) \quad (9)$$

$$u_2 = u_1 \cos \phi + w_1 \sin \phi \quad (10)$$

$$v_2 = v_1 \quad (11)$$

$$w_2 = -u_1 \sin \phi + w_1 \cos \phi \quad (12)$$

where,

$\phi$ : pitch angle in degrees, required to align  $u$  with the sloping of streamlines; and

$u_2, v_2, w_2$  are components after second rotation.

The third rotation orients 'v' perpendicular to surfaces of wind streamlines and 'w' perpendicular to streamline surfaces. The mathematical relations are as follows.

$$\psi = 0.5 \times \arctan(2\overline{v_2 w_2} / (\overline{v_2^2} - \overline{w_2^2})) \quad (13)$$

$$u_3 = u_2 \quad (14)$$

$$v_3 = v_2 \cos \psi + w_2 \sin \psi \quad (15)$$

$$w_3 = -v_2 \sin \psi + w_2 \cos \psi \quad (16)$$

where,

$\Psi$  is the final rotation; and

$u_3, v_3, w_3$  are components after final rotation

The components of wind after final rotation have been used for calculating the mean and perturbing components of wind vector. An averaging period of 5 minutes was used in the calculation of all the parameters.

Calculations of input parameters to AERMOD:

Surface Friction Velocity ( $u_*$ ):

The surface friction velocity represents the horizontal shear stress exerted by the wind vector on a horizontal surface (Van Boxel et al. 2004). It has been calculated by the following formula.

$$u_* = \sqrt{(\overline{u'w'})^2 + (\overline{v'w'})^2} \quad (17)$$

Surface Sensible Heat Flux (H): It is heat energy transferred between the ground surface and air when there is a difference in temperature between them. The sign of this heat flux indicates the direction of heat transfer. A positive value of H indicates transfer of heat energy from the ground to air and negative sign indicates the opposite. H has been calculated by the equation which shows correlation between rotated vertical wind speed and temperature (USEPA, 2004).

$$H = \rho \cdot c_p \cdot \overline{w'T'} \quad (18)$$

Where  $\rho$  is density of air and

$C_p$  is specific heat capacity of air.

Monin Obukhov length: It is the height above the ground at which the production of turbulence by both mechanical and buoyancy forces is equal. This parameter provides a measure of stability of the surface layer. Stability of the PBL is determined in AERMOD by the sign of L; Stable when  $L > 0$ , unstable when  $L < 0$  and neutral when L is very large. M.O Length has been calculated from equation (USEPA, 2004).

$$L = -(\overline{T} \cdot u_*^3) / (k \cdot g \cdot \overline{w'T'}) \quad (19)$$

where,

K is dimension less proportionality factor = 0.4;

T is the temperature and

g acc due to gravity.

Mixing Heights:

Convective ( $Z_{ic}$ ): During the day time, turbulence in the atmosphere is maintained largely by buoyant production due to solar radiation; the boundary layer is said to be in a convective state. The source of buoyancy is the upward heat flux originating from the ground heated by solar radiation. Convective turbulence is relatively vigorous and causes rapid vertical mixing in the atmospheric boundary layer.  $Z_{ic}$  is calculated with a simple one dimensional energy balance model (Carson, 1973). A modified version can be used for simplicity (Weil et al., 1997).

$$Z_{ic} = 0.3(U_* / |f|) \quad (20)$$

$U_*$  is the Surface friction velocity and

$f$  is the coriolis parameter, ( $f = 2W \cdot \sin Q$ ),

$W$  =angular velocity of earth =  $7.27 \times 10^{-5}$  rad/s,  $Q$  = latitude of the place being modeled

Applicability of equation :

Neutral PBL in mid and high latitudes, steady state & neutral conditions, absence of low level elevated inversions and cases where  $|h/L| < 1$

Convective mixing height in other conditions is calculated from the equation (Arya, 1998)

$$Z_{ic} = 0.4(U_* L / |f|) \quad (20)$$

Applicability of equation is limited to stable nocturnal boundary layer, steady state and equilibrium conditions and cases where  $|h/L| > 0$

Mechanical ( $Z_{im}$ ): At night time where, the convective mixed layer is small, the full depth of the PBL may be controlled by mechanical turbulence.  $Z_{im}$  in this case is



calculated by assuming that it approaches the equilibrium height given by Venkatram, (1992).

$$Z_{ie} = 2300.u_*^{3/2} \quad (21)$$

The  $Z_{im}$  values for each hour are calculated from the equation

$$Z_{im}\{t + \Delta t\} = Z_{im}\{t\}.e^{(-\Delta t/\tau)} + Z_{ie}\{t + \Delta t\}.(1 - e^{(-\Delta t/\tau)}) \quad (22)$$

$$\tau = Z_{im} / (\beta_\tau u_*) \quad (23)$$

where,

$Z_{im}\{t\}$  is the previous hour's value and  $Z_{im}\{t+\Delta t\}$  is present hour's value;

$u_*$  is current hour's surface friction velocity and

$\beta_\tau$  a constant with value 2

In AERMOD, the mixing height ( $Z_i$ ) is used as an elevated reflecting/penetrating surface and is determined as follows (USEPA, 2004):

$$\text{for } L < 0 (\text{CBL}) \Rightarrow Z_i = \text{Max}[Z_{ic}; Z_{im}] \quad (24)$$

$$\text{for } L > 0 (\text{SBL}) \Rightarrow Z_i = Z_{im} \quad (25)$$

Convective Velocity Scale ( $w^*$ ): A velocity scale for the layer which is used to characterize the convective portion of the CBL. The velocity scale is typically on the order of  $1 \text{ m s}^{-1}$ , which is roughly the updraft speed in convective thermals. It is calculated from the equation as (USEPA, 2004):

$$w_* = \{(gHZ_{ic})/(\rho.c_p\bar{T})\}^{1/3} \quad (26)$$

Albedo (A): The fraction of incoming solar radiation reflected back into space excluding absorption. Typical values range from 0.1 for thick dense forests to 0.9 for a surface covered with fresh snow (TCEQ, 2005). It has been calculated from the relation shown in equation (USEPA, 2004).

$$R_n = ((1 - A)R + c_1T^6 - \sigma_{SB}T^4 + c_2n)/(1 + c_3) \quad (27)$$

$R_n$ : Net radiation computed from the difference of two pyranometer readings

R: Solar radiation

$c_1$ :  $5.31 \times 10^{-13}$

$c_2$ :  $60 \text{ W/m}^2$

$c_3$ : 0.12

$\sigma_{sb}$ : stefin boltzman constant

T: ambient temperature

Bowen Ratio (Bo): The ratio of sensible heat flux to latent heat flux, or the proportion of solar radiation used to evaporate moisture from the ground and from plant and leaf surfaces. The Bowen ratio varies diurnally but is usually relatively constant during the day. Bowen ratio can range from 0.1 over water to 10.0 over desert surfaces. Bowen ratio has been calculated from the equation (USEPA, 2004).

$$H = 0.9R_n / (1 + 1/B_o) \quad (28)$$

Surface roughness: The height above the ground at which mean horizontal wind speed is zero. It is a function of land use and terrain features and varies mainly with the height of

obstacles obstructing wind flow. For this data a constant surface roughness of 0.05 was used from TCEQ guidance.

Vertical Potential Temperature Gradient: The change of potential temperature with height, used in modeling the plume rise through a stable layer, and indicates the strength of the stable temperature inversion. A positive value means that temperature increases with height above ground and indicates a stable atmosphere. For near field sampling, the values of the gradient are not expected to significantly impact the concentrations, thus were set to a minimum of 0.005.

#### References:

- Arya, S. P. 1999. *Air Pollution Meteorology and Dispersion*. New York, N.Y.: Oxford University Press.
- Carson, D. J. 1973. The development of a dry inversion-capped convectively unstable boundary layer. *Quart. J. Roy. Meteor. Soc.* 99. 450-467.
- Texas Commission on Environmental Quality (TCEQ). 2005. *AERMOD Training*.
- Van Boxel, J. H., G. Sterk, and S. M. Arens. 2004. Sonic anemometers in aeolian sediment transport research. *Geomorphology* 59: 131-147.
- Venkatram, A. 1992. Vertical dispersion of ground-level releases in the surface boundary layer. *Atmos. Environ.*, 26(A): 947-949.
- Weil, J. C., L. A. Crio, and R. P. Brower. 1997. A PDF dispersion model for buoyant plumes in the convective boundary layer. *J. Appl. Meteor.* 36: 982-1003.
- USEPA. 2004. AERMOD: Description of model formulation. EPA-454/R-03-004. Office of Air Quality Planning and Standards – Emissions Monitoring and Analysis Division. Research Triangle Park, NC.: Environmental Protection Agency.

APPENDIX C

METEOROLOGICAL DATA PROCESSING FOR FEEDLOT DATA

Meteorological data measured in the field is as shown in table C-1 (Auvermann, unpublished data, 2008).

**Table C- 1. Meteorological data collected in the field**

Date/Time	Wind Speed	Wind Direction	Solar Radiation	Air Temperature	Relative Humidity	Precipitation	Soil Temperature @ 2 m depth	Soil Temperature @ 6 m depth
	m/s	degrees	W/m <sup>2</sup>	C	%	mm	C	C
1/4/2008	5.86	52	0	8.19	0.13	0	21.73	22.28
1/4/2008	5.70	48	0	7.44	9.91	0	21.37	21.98
1/4/2008	6.38	40	0	6.16	39.72	0	21.08	21.74
1/4/2008	7.10	44	0	4.85	70.17	0	20.81	21.52
1/4/2008	7.68	42	0	3.15	98.54	0	20.52	21.33
1/4/2008	7.98	38	0	1.62	74.79	0	20.21	21.10
1/4/2008	7.27	35	0	0.77	16.00	0	19.88	20.88
1/4/2008	4.94	28	2	-0.12	25.03	0	19.55	20.65
1/4/2008	4.59	26	84	0.15	0.00	0	19.20	20.40
1/4/2008	8.42	32	276	2.94	19.67	0	19.10	20.17
1/4/2008	10.13	37	485	5.07	54.66	0	19.22	20.02
1/4/2008	8.86	37	673	7.02	16.67	0	19.59	20.00
1/4/2008	7.12	60	814	9.14	11.03	0	20.17	20.03
1/4/2008	5.90	69	890	10.44	0.28	0	20.94	20.24
1/4/2008	5.02	70	893	11.79	1.18	0	21.74	20.57
1/4/2008	3.68	76	816	12.66	3.88	0	22.49	20.96
1/4/2008	3.40	119	690	13.75	12.84	0	23.19	21.38
1/4/2008	4.41	111	514	14.31	0.00	0	23.57	21.78
1/4/2008	5.08	144	301	14.56	0.00	0	23.56	22.08
1/4/2008	5.54	146	104	13.50	0.06	0	23.28	22.25
1/4/2008	4.11	133	3	11.31	16.63	0	22.86	22.25
1/4/2008	5.26	130	0	9.63	12.78	0	22.33	22.14
1/4/2008	6.79	135	0	8.49	39.26	0	21.84	21.98
1/4/2008	6.95	131	0	7.09	37.90	0	21.41	21.76

#### Parameters used from TCEQ guidance

The following three parameters were assumed from TCEQ guidance for Deaf Smith County in Texas (TCEQ, 2005).

Albedo (A): The value of Albedo used for this data set was 0.20 which is the value prescribed by TCEQ for Deaf Smith county.

Bowen ratio ( $B_o$ ): Bowen ratio has been assumed to be 1.5 as per TCEQ guidance for Deaf Smith County in the month of April.

Surface roughness length ( $Z_o$ ): Considering the flat terrain and rural category a surface roughness of 0.05 was assumed for modeling.

#### Parameters calculated from measured data

From the field measurements the following input parameters were calculated to be given as inputs to the models:

Stability class (S): The Solar Radiation Delta-T (SRDT) method was used to define the atmospheric stability classes during the tests. Solar radiation and wind speed are the criteria used to define the atmospheric stability class according to the SRDT method (USEPA, 2000). Using these two criteria, the day time atmospheric stability class can be determined as in Table C-2. The wind speed and vertical temperature gradient are used to classify night time atmospheric stability as in Table C-3. The values for the vertical potential temperature were assumed to be constant at 0.005 (USEPA, 2004)

**Table C- 2. Estimating day time Pasquill-Gifford stability categories (USEPA, 2000)**

Wind Speed (m/s)	Solar Radiation (W/m <sup>2</sup> )			
	≥ 925	925 - 675	675 - 175	< 175
< 2	A	A	B	D
2 - 3	A	B	C	D
3 - 5	B	B	C	D
5 - 6	C	C	D	D
≥ 6	C	D	D	D

**Table C- 3. Key Estimating night time Pasquill-Gifford stability categories (USEPA, 2000)**

Wind Speed (m/s)	Vertical Temperature Gradient	
	< 0	≥ 0
< 2.0	E	F
2.0 - 2.5	D	E
≥ 2.5	D	D

Net Solar radiation ( $R_n$ ) The net radiation was estimated from the insolation and thermal radiation balance at the ground (Holtslag and van Ulden 1983). This method was adopted from EPA's AERMOD description (USEPA, 2004).

$$R_n = ((1 - A)R + c_1 T^6 - \sigma_{SB} T^4 + c_2 n) / (1 + c_3) \quad (1)$$

where,

$R_n$  is Net solar radiation;

$R$  is total solar radiation;

$A$  is the Albedo;

$c_1, c_2, c_3$  are constants with values;

$$c_1 = 5.31 \times 10^{-13};$$

$$c_2 = 60 \text{ W/m}^2;$$

$c_3 = 0.12$ ;

$\sigma_{sb}$  = Stefan Boltzmann constant ( $5.67 \times 10^{-8} \text{ W K}^{-4} \text{ m}^{-2}$ ) and

T is the ambient temperature.

Surface Sensible Heat flux (H)

H has been calculated by the following equation (USEPA, 2004).

$$H = 0.9R_n / (1 + 1/B_o) \quad (2)$$

where,

H is the sensible heat flux;

$R_n$  is the net radiation; and

$B_o$  is the Bowen ratio.

Surface friction velocity ( $u_*$ ) and Monin-Obukhov length (L): The surface friction velocity represents the horizontal shear stress exerted by the wind on a horizontal surface (Van Boxel et al., 2004). The friction velocity and the Monin Obukhov length depend on each other; thus an iterative method is used for the calculation of both parameters. An initial value of  $u_*$  is assumed for neutral conditions, from this value of  $u_*$  a value for L is calculated and then subsequent estimates of  $u_*$  and L are carried on until there is less than a 1% change between successive iterations. The expression for  $u_*$  (Panofsky and Dutton, 1984) is

$$u_* = k.u_{ref} / (\ln(z_{ref} / z_o) - \varphi_m \{z_{ref} / L\} + \varphi_m \{z_o / L\}) \quad (3)$$

where,

k is the von Karman constant (=0.4);



$u_{ref}$  is the wind speed at reference height;

$z_{ref}$  is the reference height;

$z_o$  is the surface roughness length; and

$$\varphi_m \{z_{ref} / L\} = 2 \ln((1 + v) / 2) + \ln((1 + v^2) / 2) - 2 \tan^{-1} v + \pi / 2 \quad (4)$$

$$\varphi_m \{z_o / L\} = 2 \ln((1 + v_o) / 2) + \ln((1 + v_o^2) / 2) - 2 \tan^{-1} v_o + \pi / 2 \quad (5)$$

Initially it is assumed that  $\psi_m = 0$  (neutral limit) and  $u = u_{ref}$ . From an initial estimate of  $u^*$ ,  $L$  is calculated from the definition given by USEPA, (2004) as

$$L = -(\rho \cdot C_p \cdot T_{ref} \cdot u_*^3) / (k \cdot g \cdot H) \quad (6)$$

where,

$g$  is the acceleration due to gravity ( $=9.81 \text{ m/s}^2$ );

$C_p$  is the specific heat of air at constant pressure;

$\rho$  is the density of air;

$T_{ref}$  is the ambient temperature and

$H$  is the sensible heat flux.

Mechanical mixing height ( $Z_{im}$ ) and Convective mixing height were calculated as

described in Appendix – B.

Air density ( $\rho$ ): The air density was calculated from the following equation:

$$\rho_{ma} = \frac{P_b - P_{wv}}{.37 * (t_{db} + 460)} + \frac{P_{wv}}{0.596 * (t_{db} + 460)} \quad (7)$$

where,

$\rho_{ma}$  = density of moist air ( $\text{lb/ft}^3$ ),

$P_b$  = Barometric pressure, (psia),

$P_{wv}$  = Water vapor pressure, (psia), and

$t_{db}$  = Dry bulb temperature, ( $^{\circ}$  F).

$P_{wv}$  was obtained from the following equation:

$$P_{wv} = \phi * P_s$$

$\phi$  = Relative humidity ratio (decimal form) measured in the field

$P_s$  = Saturation pressure of water vapor at dry bulb temperature (psia).

Convective velocity scale ( $W^*$ ): This parameter was calculated as described in Appendix-B.

## References

- Auvermann, B. 2008. Unpublished data:  $PM_{10}$  concentration measurements using TEOM, Amarillo, TX.: Texas AgriLife Research and Extension Center.
- Holtslag, A., and A. P. Van Ulden. 1983. A simple scheme for daytime estimates of the surface fluxes from routine weather data. *J. Appl. Meteor.* 22(4): 517–529.
- Panofsky, H. A. and J. A. Dutton. 1984. Atmospheric turbulence: Models and methods for engineering applications. New York, N.Y.: Wiley-Interscience.
- Texas Commission on Environmental Quality (TCEQ). 2005. *AERMOD Training*. Available at: [http://www.tceq.state.tx.us/files/aermet.pdf\\_4012036.pdf](http://www.tceq.state.tx.us/files/aermet.pdf_4012036.pdf).
- Van Boxel, J. H., G. Sterk, and S. M. Arens. 2004. Sonic anemometers in aeolian sediment transport research. *Geomorphology* 59: 131-147.
- USEPA. 2000. Meteorological monitoring guidelines for regulatory modeling applications. EPA-454/R-99-005. Research Triangle Park, NC.: Environmental Protection Agency, Office of Air Quality Planning and Standards Emission Factors and Inventory Group.

USEPA. 2004. AERMOD: Description of model formulation. EPA-454/R-03-004. Office of Air Quality Planning and Standards – Emissions Monitoring and Analysis Division. Research Triangle Park, NC.: Environmental Protection Agency.

## VITA

Name: Venkata Sai Vamsi Botlaguduru

Address: 324 Scoates Hall, 2117 TAMU, College Station, TX, 77843 - 2117.

Email Address: vamsi.bvs@gmail.com

Education: B.Tech, Civil Engineering, Acharya Nagarjuna University, 2007  
M.S, Biological and Agricultural Engineering,  
Texas A&M University, 2009

Affiliations: American Society of Agricultural and Biological Engineers (ASABE)